Physics – Uspekhi **46** (2) 117 – 138 (2003) ©2003 Uspekhi Fizicheskikh Nauk, Russian Academy of Sciences

REVIEWS OF TOPICAL PROBLEMS PACS numbers: 71.10.Fd, **71.27.+a**, **71.28.+d**

Short-range order in strongly correlated Fermi systems

Yu B Kudasov

DOI: 10.1070/PU2003v046n02ABEH001284

Contents

Abstract. The role of short-range order (SRO) in strongly correlated metallic systems is discussed. Magnetic neutron scattering experiments show that SRO is a universal property of such systems. Different theoretical approaches to the analysis of SRO are considered. Microscopic models based on infinite-dimensional lattice solutions (the Monte Carlo variational technique, the $1/D+1/D^2$ expansion for the Gutzwiller trial wave function, and the dynamical mean-field theory) do not correctly describe SRO in strongly correlated systems. A variational theory of SRO in Fermi systems is presented in which, in addition to Gutzwiller's variational parameter, a set of new parameters describing nonlocal short-range correlations is used.

1. Introduction

Short-range order (SRO) in the arrangement of particles has been studied for a fairly long period both in classical systems, e.g., in the theory of liquid, and in quantum systems, e.g., in the Ising model [1]. In recent decades the interest in this problem has intensified because of active studies of strongly correlated Fermi systems in condensed media. Strong electron correlations lead to various physical phenomena, such as metal – insulator phase transitions [2], states with heavy fermions [3], high-temperature superconductivity [4], etc. With all the diversity of strongly correlated Fermi systems, dynamical SRO is one of the universal properties whose study is needed in order to understand the nature of the strongly correlated state. The last two decades have seen considerable progress in experimental studies of short-range nonlocal correlations of electrons in condensed media by the magnetic neutron scattering method [5, 6] which provides the means for studying the SRO structure in great detail.

The goal of this review is to analyze the role that SRO plays in the formation of a strongly correlated state. By short-range antiferromagnetic (AFM) order we mean strong AFM correlations encompassing one or several unit cells, i.e., a small number of nearest neighbors. In metallic systems, SRO is of a dynamic nature, in contrast to static SRO, e.g., in spin glass. We call a state in which strong AFM correlations extend over much greater, but still microscopic, distances, e.g., $\sim 10-100$ unit cells, a frustrated antiferromagnet. In contrast to strong SRO, in a frustrated antiferromagnet the topology of the lattice and scaling play an important role, and these two factors have led to the development of specific methods of investigation (e.g., see Ref. [7]), which we will not discuss here.

The main aspects of strongly correlated Fermi systems can be studied with the Hubbard model (see the reviews in Refs [4, 8 – 12]). Several general analytical approaches exist here. The Hubbard model has an exact solution [13] and well-developed analytical methods for a one-dimensional (1D) chain [14, 17]. The opposite limit, an infinite-dimensional lattice ($D=\infty$), has also been thoroughly studied, and here an almost exact solution for the ground state with $D=\infty$ is provided by Gutzwiller's variational method [15]. In the $D=\infty$ limit, the

Yu B Kudasov Russian Federal Nuclear Center—VNIIÉF
Prosp. Mira 37, 607188 Sarov, Nizhniĭ-Novgorod Region,
Russian Federation
Tel. (+7-83130) 455 84
Fax (+7-83130) 453 84
E-mail: kudasov@ntc.vniief.ru

Received 17 July 2002
Uspekhi Fizicheskikh Nauk **173** (2) 121 –144 (2003)
Translated by E Yankovsky; edited by M V Magnitskaya

nonlocal correlations between the fermions can be replaced by a mean field, while only the intrasite correlations remain dynamic [16, 18]. Note that the dynamical mean-field theory is based on this fact [12]. Solutions for lattices of intermediate dimensionalities, e.g., for 2D and 3D lattices (which are of great practical importance), have proved to be more complicated [19–22], primarily because of the development of nonlocal correlations.

Short-range order in solids also emerges because of the interaction between itinerant electrons and localized electronic states [3]. Of special interest here are the periodic lattices of localized electrons, or concentrated Kondo systems (Kondo lattices). The presence of special quasiparticle (coherent) states was discovered in such systems, namely, heavy fermions which have huge effective masses of order 10^2-10^3 free electron mass. In almost all systems with heavy fermions the presence of SRO was detected.

Section 2 establishes, on the basis of an analysis of the experimental data, the main features of SRO in various strongly correlated systems. In Section 3 we will briefly discuss the phenomenological theories and the mean-field theories of strong nonlocal correlations. Section 4 is devoted to a thorough exposition of the variational theory of SRO in molecules and crystalline substances. Finally, in Section 5 we will formulate the main conclusions.

2. Experimental investigation of SRO in strongly correlated metallic systems by the magnetic neutron scattering method

2.1 Magnetic neutron scattering

Spin fluctuations on the whole and SRO in particular have an effect on the kinetic and thermodynamic properties of substances, such as conductivity, specific heat, static magnetic susceptibility, etc. [23]. However, the integral characteristics alone do not make it possible to determine the SRO structure unambiguously, i.e., to determine the correlation length, the magnetic excitation spectrum, etc.

The dipole interaction between the neutrons and the magnetic moments in solids leads to magnetic scattering of these neutrons. The energy and wave vector of thermal and cold neutrons are closely matched to the characteristic energies and wavelengths of the magnetic excitations in solids, so that neutron scattering is one of the main methods of studying magnetic order, including SRO. This method makes possible direct probing of spin fluctuations and is a powerful instrument for studying the SRO structure in strongly correlated systems.

The cross section of magnetic neutron scattering with momentum transfer $\hbar\mathbf{q} = \hbar(\mathbf{k} - \mathbf{k}')$ and energy transfer $\hbar\omega$ can be expressed as follows [5]:

$$\frac{\mathrm{d}^2\sigma}{\mathrm{d}\Omega\,\mathrm{d}E'} = \frac{k'}{k}\left(\frac{\gamma r_0}{2}\right)^2 \left[f(\mathbf{q})\right]^2 \exp\left[-2W(\mathbf{q})\right] \times \sum_{\alpha\beta}(\delta_{\alpha\beta} - \tilde{q}_\alpha\tilde{q}_\beta)\, N\mathcal{S}^{\alpha\beta}(\mathbf{q},\omega)\,, \tag{1}$$

where $f(\mathbf{q})$ is the magnetic form factor, $\exp[-2W(\mathbf{q})]$ is the Debye–Waller factor, $\tilde{q}_\alpha$ is the unit vector along $\mathbf{q}$, α and β are indices denoting the Cartesian components of a vector, N is the number of magnetic ions, and $\gamma r_0/2 = 7.265\times10^{-2}$ barn μ_B^{-2} in units adopted in Ref. [5]. The dynamical structure factor is given by the following formula [5]:

$$\mathcal{S}^{\alpha\beta}(\mathbf{q},\omega) = \frac{g\mu_\mathrm{B}}{2\pi\hbar N}\sum_{\mathbf{R},\mathbf{R}'}\int \mathrm{d}t \exp\left\{\mathrm{i}\left[\omega t - \mathbf{q}(\mathbf{R}-\mathbf{R}')\right]\right\} \times \left\langle S^\alpha_\mathbf{R}(t)\, S^\beta_{\mathbf{R}'}(0)\right\rangle, \tag{2}$$

where g is the Lande factor, $S^\alpha_\mathbf{R}(t)$ is the α Cartesian projection of spin of the ion with the position vector $\mathbf{R}$ at time t, and $\langle\ldots\rangle$ stands for a thermal average. The factor $\delta_{\alpha\beta} - \tilde{q}_\alpha\tilde{q}_\beta$ reflects the fact that the neutrons probe the spin projection that is perpendicular to the momentum transferred. When spin-space anisotropy can be ignored, this factor is replaced by 2. Formula (2) shows that the dynamical structure factor contains all the information about spin correlations. This factor is related to the imaginary part of the dynamic spin magnetic susceptibility through the fluctuation-dissipation theorem [5]:

$$\mathcal{S}(\mathbf{q},\omega) = \frac{\chi''(\mathbf{q},\omega)}{\pi\left[1-\exp(-\hbar\omega/k_\mathrm{B}T)\right]}\,. \tag{3}$$

The real part of the magnetic susceptibility can be found by using the Kramers–Kronig relation:

$$\chi'(\mathbf{q},\omega) - \chi'(\mathbf{q},\infty) = \frac{1}{\pi}\int_{-\infty}^{\infty}\mathrm{d}\omega\,\frac{\chi''(\mathbf{q},\omega')}{\omega'-\omega}\,. \tag{4}$$

There is one more characteristic of neutron scattering that is often used, the intensity $I(\mathbf{q},\omega) = 2(\gamma r_0/2)^2[f(\mathbf{q})]^2\times \mathcal{S}(\mathbf{q},\omega)\exp[-2W(\mathbf{q})]$. Here it is also given in units adopted in Ref. [5].

Rossat-Mignod et al. [6] proposed a method for separating the dynamic magnetic susceptibility into two components, one originating from local spin correlations (electrons on the same ion), and the other originating from nonlocal correlations (electrons at different lattice sites). In the first case, the correlation function $\langle S_1(R)\,S_2(R')\rangle$ is a delta function in the coordinate space, whereby in the momentum representation the Fourier transform of the correlation function is independent of the wave vector. Thus, the analysis of the experimental results is reduced to the following. First, the background intensity is removed from the neutron scattering intensity. Then, the constant and $\mathbf{q}$-dependent parts of the scattering intensity are separated. Accordingly, two terms appear in the dynamic magnetic susceptibility. In the simplest case they can be described as follows [5, 24]:

$$\chi''_\mathrm{SS}(\omega) = \chi_\mathrm{SS}\,\frac{\omega\Gamma_\mathrm{SS}}{\omega^2+\Gamma_\mathrm{SS}^2}\,, \tag{5}$$

$$\chi''_\mathrm{IS}(\omega) = \frac{\chi_\mathrm{IS}}{1+(q/\varkappa)^2}\,\frac{\omega\Gamma_\mathrm{IS}(\mathbf{q},\omega)}{\omega^2+\Gamma_\mathrm{IS}^2(\mathbf{q},\omega)}\,, \tag{6}$$

where SS and IS denote the local (site–site) and nonlocal (intersite) contributions to the dynamic susceptibility, and $\varkappa$ is the inverse correlation length. Equations (5) and (6) are a reflection of the hypothesis that the decay of correlations in time and space follows an exponential law and, therefore, are fairly general: the expressions for the dynamic spin susceptibility in the random-phase approximation (RPA) and the spin-fluctuation theory (SFT) assume the form of equations (5) and (6) [23].

2.2 Transition 3d-metal compounds: V_2O_3 and LiV_2O_4

Vanadium sesquioxide (V_2O_3), related solid solutions with chromium and titanium sesquioxides, and compositions with an oxygen excess or deficit comprise one of the basic families of materials long employed to study Coulomb correlations and Mott–Hubbard phase transitions [2]. These compounds have a complex phase diagram. The regions of paramagnetic (PM) insulator, AFM insulator, and PM metal are separated by first-order phase transitions [2, 25, 26].

Brinkman and Rice [27] studied the metallic phase of V_2O_3 and were the first to show that strong correlations narrow the quasiparticle band. This leads to the main attributes of a strongly correlated metallic state, i.e., a rapid increase of the linear term of the electron specific heat (γT) and the static magnetic susceptibility [27]. In the last decade, many aspects of the strongly correlated state in vanadium sesquioxide have been seriously reviewed. In 1993, Bao et al. [28] found that near $T = 0$ K in the metallic phase there exists a state with an incommensurate spin-density wave (SDW). Later, Park et al. [29] found that two 3d electrons of the V^{3+} ion are basically on the twofold degenerate orbitals e_g in the state with $S = 1$ (instead of in the state with $S = 1/2$, which was assumed to be the case earlier). Thus, the electron subsystem of V_2O_3 can be described by the twofold degenerate Hubbard model.

A thorough study of the ground state and spin correlations in the metallic PM phase and the PM and AFM insulator phases of the single-crystal V_2O_3 has been conducted by Bao et al. [5, 30]. Figure 1 shows the intensity of neutron scattering in the metallic PM phase of V_2O_3 at temperatures somewhat higher than the AFM–PM transition point ($T = 200$ K). There are two broad peaks in the (1 0 0) and (1 0 2.1) directions (in the basis of the conventional hexagonal cell with six V_2O_3 formula units), which are related to short-range electron correlations. These directions coincide with the SDW directions in $V_{2-y}O_3$ at $T = 0$ K. The peaks at (1 0 0) and (1 0 2.1) disappear in the transition to the AFM phase at $T < 170$ K, as Fig. 1 clearly shows. Injection of excess oxygen into vanadium sesquioxide stabilizes the metallic phase down to 0 K, whereby nonstoichiometric compositions can be used to study the temperature dependence of the peak height and halfwidth. The results of these measurements at temperatures above SDW ordering are shown in Fig. 2. In Ref. [5] they are discussed in the framework of the scaling hypothesis in SFT as the SDW phase is approached. There is a certain factor that should be mentioned at this point. If we use Fig. 2 to estimate the correlation length $\varkappa^{-1}$, we get values ranging from 6 to 2 Å. It is hardly possibly to speak of scaling for the correlation length over distances of the order of, or smaller than, the interatomic separation. For a meaningful description we would need a microscopic theory of short-range order.

To analyze the effect of stoichiometry on short-range order, the neutron scattering intensities for V_2O_3 and $V_{2-y}O_3$ (at $y = 0.027$) were compared. The second composition is highly nonstoichiometric, since the AFM phase is completely suppressed already at $y \approx 0.015$. Nevertheless, the intensities of scattering by magnetic fluctuations for the two compositions were practically the same, i.e., SRO proved to be only slightly sensitive to stoichiometry and doping by chromium sesquioxide. Another characteristic feature established by

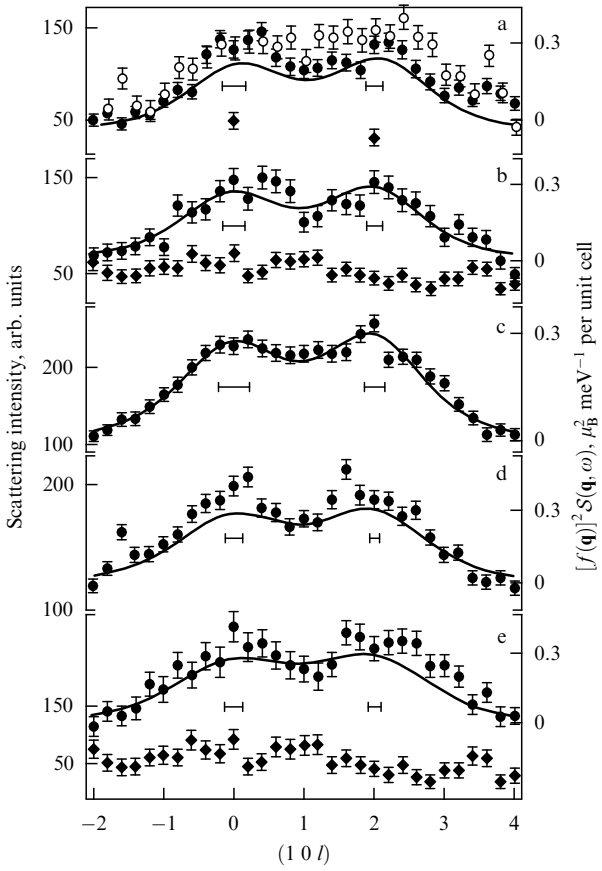

Figure 1. Intensity of neutron scattering along the direction (1 0 l) for different values of energy transfer: (a) $\hbar\omega = 6$ meV, (b) $\hbar\omega = 9$ meV, (c) $\hbar\omega = 12$ meV, (d) $\hbar\omega = 18$ meV, and (e) $\hbar\omega = 25$ meV. Solid circles indicate the data for V_2O_3 in the PM phase at $T = 200$ K, solid diamonds, the data for V_2O_3 in the AFM phase at $T = 160$ K, and open circles, the data for $V_{1.973}Cr_{0.027}O_3$ in the PM phase at $T = 200$ K (after Ref. [5]).

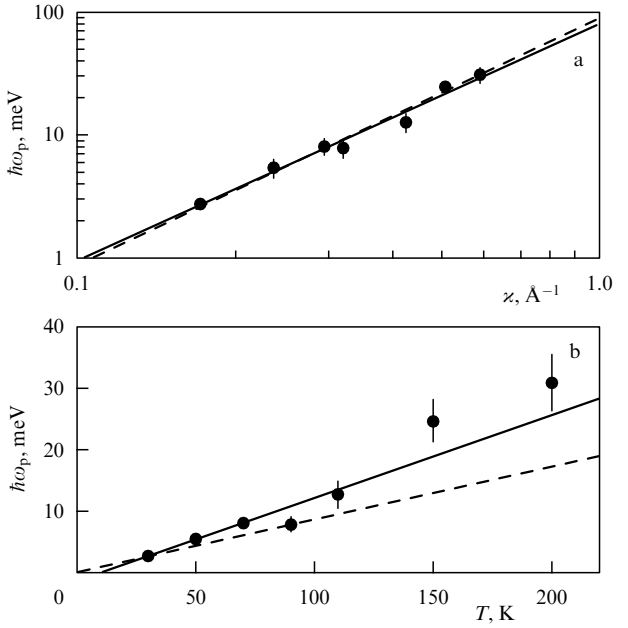

Figure 2. Dependence of the energy of the peak in imaginary part of the dynamic spin susceptibility for $V_{1.973}O_3$ in the PM phase on the inverse correlation length $\varkappa$ and temperature [5]. (a) The solid line is the best fit of the dependence of the energy of the peak, $\hbar\omega_p \propto \varkappa^z$, where $z = 1.9$, and the dashed line is the best fit with $z = 2$. (b) The solid line is the best fit for the linear dependence of the peak's energy on temperature, which roughly corresponds to the thermal energy $k_B T$ (dashed line).

Bao et al. [5] is the universal nature of the profile of the peak dynamic magnetic susceptibility as a function of energy in terms of normalized units. Here the absolute values of the energy at which the maximum occurs and the absolute values of the peaks in dynamic susceptibility were found to differ significantly. Strong short-range correlations were also observed in the PM insulator phase [$(V_{1.972}Cr_{0.028})_2O_3$ at $T = 205$ K]. On the whole the correlations were similar to those observed in the metallic PM phase. Figure 3 shows the energy dependence of the imaginary part of the magnetic susceptibility, χ'', in the metallic PM phase for the wave vector $\mathbf{q} = (1\,0\,2.1)$, and of χ'' averaged over $\mathbf{q}$ [see equation (5)]. Such separation makes it possible to estimate the parameters of local and nonlocal correlations (Table 1).

Of all the transition 3d-metal compounds, LiV_2O_4 has the greatest value of the Sommerfeld constant, $\gamma = 430$ mJ mol^{-1} K^{-2} [31 – 33], which places the electron system of LiV_2O_4 on the same level with heavy-fermion compounds. Since the time of the discovery of a strongly correlated state in this substance, extensive theoretical and experimental research has been conducted [32]. There are different viewpoints concerning the nature of this state. According to one, LiV_2O_4 is a Kondo lattice without f-ions. The half-filled singlet state a_{1g} is assumed to be localized, while the e_g-doublet forms the conduction band [34]. According to another view, structural frustration of magnetic order, which hinders the development of long-range AFM order, plays the leading role [32]. Fulde et al. [35] went even farther and assumed that the frustration itself is the source of the strongly correlated state.

Lee et al. [36] studied the neutron scattering on polycrystalline LiV_2O_4. At temperatures below 30 K a peak in the q-dependence of the dynamic susceptibility emerges at 0.64 Å^{-1} (or $0.84\,a^*$ in units of the reciprocal lattice constant), and this peak is related to the development of short-range order. Note that according to the results of conductivity and magnetic susceptibility measurements, this temperature corresponds to the emergence of a strongly correlated state. The halfwidth and height of the peak are strongly temperature dependent. Here the halfwidth proves to be an almost perfect linear function of the temperature.

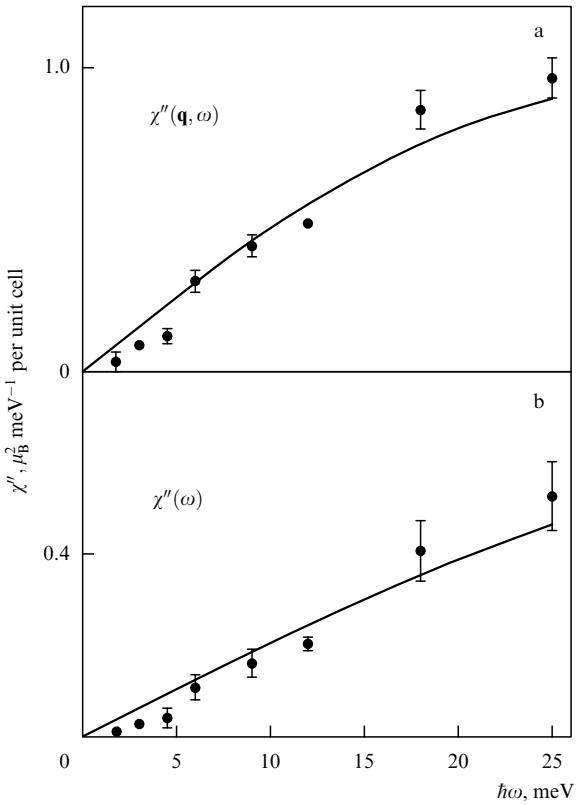

Figure 3. Imaginary part of the dynamic spin susceptibility of V_2O_3 at $T = 200$ K: $\mathbf{q} = (1\,0\,2.1)$ (a), and independent of $\mathbf{q}$ (local) component (b) [5].

Recently, Fulde et al. [35] assumed that the crystal structure of LiV_2O_4 in the form of tetrahedrons with common vertices leads to disruption of charge order and formation of specific structures (rings and chains of finite

Table 1. Magnetic excitations and SRO in strongly correlated compounds (γ is the Sommerfeld constant, $\mathbf{q}$ and ω_0 are the wave vector and excitation energy, ξ is the correlation length, and $\Gamma_{SS\,(IS)}$ is the rate of relaxation of intra- (inter-) site magnetic excitations).

Composition	γ, mJ mol^{-1} K^{-2}	$\mathbf{q}$	ξ, Å	ω_0, meV	Γ_{SS}, meV	Γ_{IS}, meV
V_2O_3	40 [2]	(1 0 0)	≈ 2 ($T = 200$ K) [5]*	≈ 35 ($T = 200$ K) [5]*	> 35 ($T = 200$ K) [5]*	≈ 15 meV ($T = 200$ K) [5]*
LiV_2O_4	430 [32]	0.64 Å^{-1}	6 ($T = 1.4$ K) [36]	1 ($T = 1.4$ K) [36]		1.42 ($T = 1.4$ K) [36]
$CeCu_6$	≈ 1500 [37]	(0 0 1) (0.85 0 0)	$\xi_a = 9 \pm 1$ $\xi_c = 3.5 \pm 0.5$ ($T = 0$ K) [6]	0.3 ($T = 0$ K) [6]	0.4 ($T = 0$ K) [6]	0.2 ($T = 0$ K) [6]
$CeRu_2Si_2$	350 [24]	(0.31 0.31 0)	12.5 (3a)** ($T = 1.5$ K) [24]	1.2 ($T = 1.5$ K) [24]	2 ($T = 1.5$ K) [24]	0.75 ($T = 1.5$ K) [24]
$Ce_{1-x}La_xRu_2Si_2$	600 [24]	(0.31 0.31 0)	19 (4.5a)** ($T = 1.5$ K) [24]	0.2 ($T = 1.5$ K) [24]	1.4 ($T = 1.5$ K) [24]	0.2 ($T = 1.5$ K) [24]

* Estimated by the author.
** In parentheses is the value in lattice constant units.

length of spin 1/2 and 1). In this case, SRO in LiV_2O_4 must differ from ordinary AFM correlations. In particular, the expected peak value of the dynamic susceptibility must occur at $q = \sqrt{2}a^*$, which does not correspond to the value observed in the experiments of Lee et al. [36]. Thus, apparently in LiV_2O_4 there is ordinary short-range AFM order.

2.3 Heavy fermions: $CeCu_6$ and $Ce_{1-x}La_xRu_2Si_2$

The $CeCu_6$ compound, on the one hand, has one of the highest values of the Sommerfeld constant ($\gamma \approx 1500$ mJ mol^{-1} K^{-2} [37]) among metallic systems and remains nonmagnetic down to very low temperatures (indications of AFM order have been discovered only at $T \leqslant 2$ mK [38]) and, on the other hand, is one of the most thoroughly studied substances with heavy fermions. There have already been in-depth studies of SRO in $CeCu_6$ and its dependence on temperature, doping, and magnetic field [6, 39]. Neutron scattering has been investigated along the crystallographic directions (1 0 0) and (0 0 1) and it was found that the magnetic correlations in $CeCu_6$ are highly anisotropic. At $T \to 0$ K the correlation lengths are $\xi_a = (9 \pm 1)$ Å and $\xi_c = (3.5 \pm 0.5)$ Å. Thus, along direction **a** SRO encompasses the next-to-nearest neighbors, while along **c** it encompasses only the nearest neighbors. What was also discovered was an essentially anisotropic peak on the incommensurate wave vector, which suggests that there is competition between the magnetic interactions along the **a** axis. Figure 4a shows the temperature dependence of the anisotropic correlation length. The development of SRO at low temperatures is very evident. Note that emergence of SRO coincides with the emergence of heavy fermions (according to thermodynamic and magnetic measurements [40]). The spin-excitation relaxation rates were also estimated: $\Gamma_{SS} = 0.4$ meV and $\Gamma_{IS} = 0.2$ meV as $T \to 0$ K. These rates rapidly increase with temperature: at $T = 3$ K they become $\Gamma_{SS} = \Gamma_{IS} = 0.6$ meV (Fig. 4b). On the whole, other heavy-fermion compounds, such as UPt_3 [40, 41–43], $CeRu_2Si_2$ [6, 44], and U_2Zn_{17} [45], demonstrate similar behavior.

The results of experiments on neutron scattering by spin fluctuations in $CeCu_6$ in strong magnetic fields can be found in Refs [39, 40]. The magnetic field suppresses SRO, with the weakening of SRO in this case agreeing with the disappearance of heavy fermions in a magnetic field, determined through specific-heat measurements [40]. Figure 5 shows the linear term in the specific heat, C/T, and the magnetic susceptibility, $\chi(\mathbf{q}, 0)$, as functions of the magnetic field strength.

Two processes compete in heavy-fermion compounds. On the one hand, the interaction between localized states and itinerant electrons leads to the formation of Kondo singlets, with the result that the impurities are 'screened' and a transition to the nonmagnetic state takes place. On the other hand, the interaction of localized states via itinerant electrons, or the Rudermann–Kittel–Kasuya–Yosida (RKKY) interaction, tends to transfer the system to an ordered magnetic state. Thus, many heavy-fermion systems ($CeCu_6$, $CeRu_2Si_2$, and others), while being nonmagnetic, are still close to the transition to the AFM state on Doniach's diagram [47]. In this case the transition to the ordered AFM phase may be initiated by applying pressure or by adding impurities. For instance, in the $Ce_{1-x}La_xRu_2Si_2$ compound, the critical concentration at which long-range AFM order emerges is $x = 0.075$. To analyze the critical behavior of the spin correlations near the transition point, Raymond et al. [24] and Kambe et al. [48] studied the dependence of the neutron scattering spectra in $Ce_{1-x}La_xRu_2Si_2$ on the lanthanum concentration. It was found that even for the critical composition the correlation length amounts only to two-to-four unit cell sizes. Similar results for the critical behavior of spin correlations were achieved by von Löhneysen [49] when gold was substituted for copper in $CeCu_6$.

2.4 High-temperature superconductors

High-temperature superconductors with two-dimensional CuO_2 planes exhibit strong and fairly unusual short-range AFM correlations which substantially affect the properties of these substances [4, 8, 10]. The magnetic interactions of the holes (electrons) in the CuO_2 planes are interpreted as constituting one of the possible mechanisms of high-temperature superconductivity [4, 10]. Moreover, AFM fluctuations are assumed to be the reason for the pseudogap behavior of high-temperature superconductors in the normal phase [50]. This explains the extensive investigations of magnetic excitations and correlations done with these substances. A detailed discussion of the various aspects of this problem can be found in review articles (e.g., see Refs [4, 10, 50–52]). The results

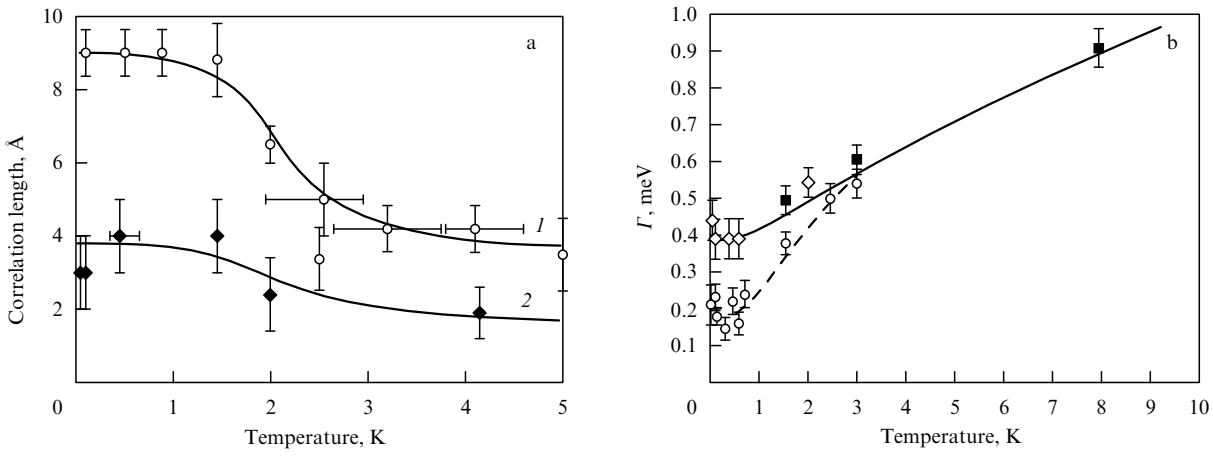

Figure 4. SRO in $CeCu_6$ (according to Ref. [6]). (a) Anisotropic correlation length. Open circles and curve *1* represent correlations along the **a** axis, while solid diamonds and curve *2* represent correlations along the **c** axis. (b) Decay rates of intrasite correlations, Γ_{SS} (open diamonds and solid curve), and of intersite correlations, Γ_{IS} (open circles and dashed curve). The solid squares represent the results of time-of-flight experiments [46].

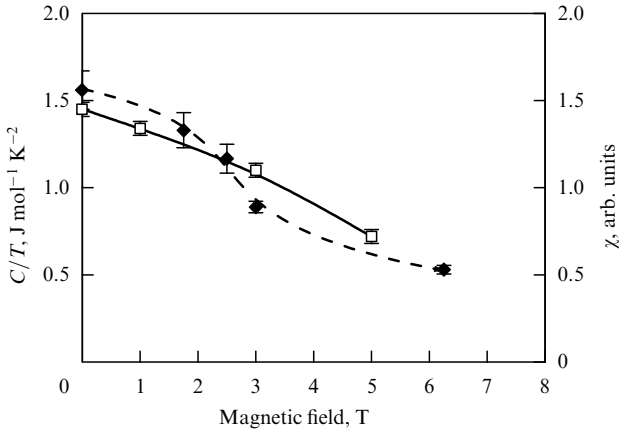

Figure 5. SRO in $CeCu_6$ in a magnetic field: the imaginary part of the static magnetic susceptibility $\chi(\mathbf{q}, 0)$ at $\mathbf{q} = (1.4\ 0\ 0)$ [39, 40] (solid diamonds), and the specific heat C/T [40] (open squares).

obtained for different substances ($La_{2-x}Sr_xCuO_4$, $YBa_2Cu_3O_{7-x}$, and others) clearly exhibit general pronounced regularities. The doping of the initial AFM insulator with holes (electrons) leads to the destruction of AFM order and to transition to the metallic state. However, if the number of mobile charge carriers is moderate (underdoped regime), the metallic phase exhibits strong AFM correlations with a large correlation length [51]. When the transition to the metallic state occurs, the peak in the intensity of scattering on the AFM wave vector (π, π) weakens or disappears altogether. At the same time, peaks caused by SRO appear on the incommensurate wave vectors $(\pi, \pi) + \delta(\pi, 0)$ and $(\pi, \pi) + \delta(0, \pi)$, where δ is the incommensurability parameter [51]. Interestingly, the dependence of δ on the dopant concentration x for La_2CuO_4-based compounds for different dopants approximately follows the doping dependence of the superconducting transition temperature [51]. As the concentration increases, the magnetic correlation length rapidly decreases, e.g., as $x^{-1/2}$ for $La_{2-x}Sr_xCuO_4$ [52]. Under optimal doping, i.e., when the superconducting transition temperature is at its maximum, the correlation length extends over two-to-three unit cells [51]. It must also be noted that in the superconducting state there is a sharp peak in the spin fluctuation spectrum of $YBa_2Cu_3O_{7-x}$, $Bi_2Sr_2CaCu_2O_{8+x}$, and $Tl_2Ba_2CuO_{6+x}$, a peak that disappears completely in the normal state [53, 54]. This phenomenon suggests that there is a close relationship of the high-temperature superconductivity in cuprates with spin fluctuations and short-range AFM order.

2.5 The nearly antiferromagnetic alloy $Cr_{1-x}V_x$

The above examples show that a strongly correlated state is accompanied by the emergence of low-energy spin fluctuations interpreted as a consequence of SRO. The increase in the Sommerfeld constant γ and the static (dynamic) magnetic susceptibility in strongly correlated compounds can be explained by the narrowing of the quasiparticle band, which is accompanied by a decrease in the energy of spin excitations and the rate of their relaxation. This pattern has indeed been established on the basis of the data listed in Table 1.

On the other hand, one can also pose the opposite question: is the emergence of low-energy spin excitations in an electron system a sufficient condition for the existence of a strongly correlated state? Generally the answer is no. As an example, let us take an ordinary AFM metal in which there is no strong renormalization of the effective mass, e.g., chromium. By doping with vanadium we can suppress the long-range AFM order. The critical composition of $Cr_{1-x}V_x$ is the one with $x = 0.035$. As we approach the critical value of x from the side of the PM phase, spin correlations develop in the alloy, but no strongly correlated state emerges. Nevertheless, Fawcett et al. [55] discovered low-energy spin excitations in $Cr_{0.95}V_{0.05}$ in the PM phase. It was found that the renormalization of the dynamic magnetic susceptibility which was estimated on the basis of a comparison of the experimental results with the results of band structure calculations, may be as high as 28. However, in contrast to other strongly correlated systems, the strongly renormalized low-energy excitations in $Cr_{0.95}V_{0.05}$ exist only within a narrow range of $\mathbf{q}$ near six points in the Brillouin zone: $(1 \pm \delta\ 0\ 0)$, $(1 \pm \delta\ 0)$, and $(1\ 0 \pm \delta)$. Further measurements for high energy transfer values showed that spin excitations actually exist within a broad energy range (at least up to 400 meV) near the (1 0 0) direction [56]. This led Hayden et al. [56] to believe that the relaxation time Γ^{-1} averaged over the Brillouin zone, or $\Gamma_{\rm av}^{-1}$, may serve as a criterion for the emergence of a strongly correlated state. The simple idea that spin excitations are a set of oscillators suggests that [56]

$$\gamma = \frac{\pi k_{\rm B}}{\hbar}\,\frac{1}{\Gamma_{\rm av}} = \frac{\pi k_{\rm B}}{\hbar}\left\langle \frac{1}{\Gamma_{\rm IS}(\mathbf{q})} \right\rangle_{\rm BZ}, \qquad (7)$$

where $\langle \ldots \rangle_{\rm BZ}$ stands for a Brillouin-zone average. In the case of $Cr_{0.95}V_{0.05}$, the low-energy excitations encompass a very small part of the Brillouin zone and therefore cannot have a marked effect on the Sommerfeld constant. Figure 6 shows the dependence (7) and the position of various substances with strong correlations in the $(\gamma, \Gamma_{\rm av})$ plane.

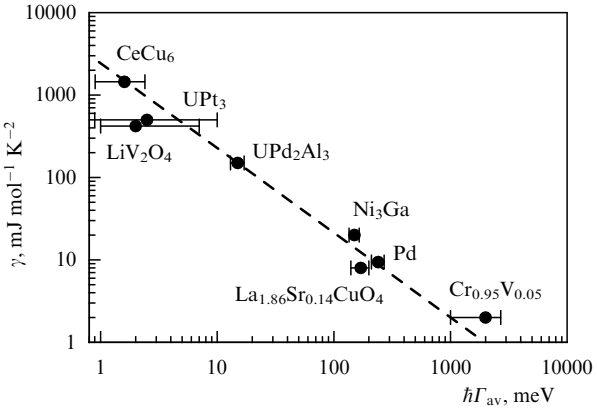

Figure 6. Sommerfeld constant as a function of the averaged relaxation rate $\Gamma_{\rm av}$ (according to Ref. [56]; $\Gamma_{\rm av}$ for LiV_2O_4 was estimated by the present author on the basis of the data of Ref. [36]). \

2.6 General trends

The parameters characterizing SRO for some strongly correlated substances are listed in Table 1. The following conclusions can be drawn on the basis of the experimental results discussed above:

(a) The energy of the spin relaxations related to SRO and the relaxation rate of these excitations decrease with increasing effective mass of the mobile charge carriers. This agrees well with the idea about the narrowing of the quasiparticle band.

(b) Strong short-range correlations cannot be interpreted as quasiparticle excitations, since their relaxation rate is comparable to the excitation energy and they are localized in coordinate space within several unit cells. In other words, the energy and momentum of these excitations are not 'good' quantum numbers.

(c) The development of a strongly correlated state is almost always accompanied by the appearance of SRO. The suppression of the strongly correlated state by raising the temperature, applying an external magnetic field, adding impurities, etc. leads to the disappearance of SRO, which points to the close relationship between these two phenomena. This statement is most important, since it shows that explaining the nature of the strongly correlated state requires stepping outside the scope of the theoretical $D = \infty$ models, where there cannot be any SRO.

(d) High-temperature superconductors comprise a special group. In them even a moderate renormalization of the effective mass leads to an anomalously large AFM correlation length in the metallic phase, notwithstanding the quasi-two-dimensional nature of magnetic interactions.

3. Phenomenological SRO theories and mean-field theories

3.1 Mean-field theories and spin-fluctuation theory

It is convenient to begin the analysis of spin fluctuations in correlated systems with the Hubbard model. In the case of a single nondegenerate band, this model can be formulated in terms of the following Hamiltonian:

$$H = \sum_{ij,\sigma} t_{ij} a_{i\sigma}^{+} a_{j\sigma} + U \sum_{i} n_{i\uparrow} n_{i\downarrow} , \tag{8}$$

where $a_{i\sigma}^{+}$ ($a_{i\sigma}$) is the operator of creation (annihilation) of a fermion with spin $\sigma = \uparrow, \downarrow$ at the ith lattice site, and $n_{i\sigma} = a_{i\sigma}^{+} a_{i\sigma}$. In the static mean-field approximation, the spectrum of the elementary magnetic excitations ($a_{\mathbf{k}\uparrow}^{+} a_{\mathbf{k}+\mathbf{q}\downarrow}$) is determined by the expression $\varepsilon_{\mathbf{k},\mathbf{q}} = 2\Delta + \varepsilon_{\mathbf{k}} - \varepsilon_{\mathbf{k}+\mathbf{q}}$, where the term 2Δ is related to exchange splitting of the band. The dynamic (spin) susceptibility corresponding to this spectrum has the form [23, 57]

$$\chi_{\Delta 0}^{+-}(\mathbf{q}, \omega) = \sum_{\mathbf{k}} \frac{f(\varepsilon_{\mathbf{k}+\mathbf{q}} - \Delta) - f(\varepsilon_{\mathbf{k}} + \Delta)}{\varepsilon_{\mathbf{k}} - \varepsilon_{\mathbf{k}+\mathbf{q}} + 2\Delta - \omega} , \tag{9}$$

where $f(\varepsilon)$ is the Fermi distribution function.

The next step is the inclusion of mean-field fluctuations in time. Such an approximation is known as the dynamic mean-field approximation, or the random-phase approximation (RPA). This leads to an important result, the enhancement of the dynamic susceptibility due to spin fluctuations [23, 57]:

$$\chi_{\mathrm{RPA}}^{+-}(\mathbf{q}, \omega) = \frac{\chi_{\Delta 0}^{+-}(\mathbf{q}, \omega)}{1 - I\chi_{\Delta 0}^{+-}(\mathbf{q}, \omega)} , \tag{10}$$

where $I = U/L$, with L being the number of lattice sites.

One drawback of RPA is the absence of an inverse effect of the strongly renormalized spectrum of spin fluctuations on the thermodynamic potential. This drawback manifests itself most vividly at finite temperatures. To eliminate it, a special theory of self-consistent renormalization of spin fluctuations has been developed [23]. To obtain a self-consistent description, one can start from the formally exact relation for the free energy of a system of interacting fermions. For a Hamiltonian of a sufficiently general form $H = \sum_{\mathbf{k}} \varepsilon_{\mathbf{k}} n_{\mathbf{k}} + H_1(I)$, where I is the coupling parameter, the free energy can be written as follows [23]:

$$F(M, T) = F_{\mathrm{HF}}(M, T) + \Delta F(M, T) , \tag{11}$$

$$\Delta F(M, T) = -T \sum_{m} \sum_{\mathbf{q}} \int_0^I \mathrm{d}\lambda \left[\chi_{M\lambda}^{+-}(\mathbf{q}, \mathrm{i}\omega_m) - \chi_{M0}^{+-}(\mathbf{q}, \mathrm{i}\omega_m) \right],$$

where M and T are the magnetic moment of the system and the temperature, $\omega_m = 2\pi m T$ are the Matsubara frequencies, m is an integer, and $\chi_{M\lambda}^{+-}$ is the dynamic susceptibility at a fixed M and for $I = \lambda$.

Expression (11) makes it possible to step outside RPA. Different approaches are used to analyze Eqn (11) in the cases of weak ferromagnetism (the long-wave approximation), a nearly ferromagnetic metal, etc. [23]. The self-consistent spin renormalization theory enables many characteristics of the medium affected by spin fluctuations, such as specific heat, thermal expansion, electrical conductivity, dynamic susceptibility, etc. to be consistently described with the use of only a small set of parameters. The general form of the dynamic susceptibility remains the same as in RPA [Eqn (10)]. Useful formulas for analyzing the results of inelastic neutron scattering by spin fluctuations have been derived in the self-consistent spin renormalization theory [48]:

$$\Gamma_{\mathrm{IS}} = 2\pi T_0 y , \tag{12}$$

$$\frac{\xi}{a} = 0.27 y^{-1/2} , \tag{13}$$

where T_0 is the characteristic energy of spin excitations, y is the reciprocal static magnetic spin susceptibility on the AFM-order wave vector, and a is the size of the unit cell. Note, for instance, that at low temperatures the contribution of magnetic fluctuations to the specific heat is described by the same set of parameters [48]:

$$\frac{C_m}{T} \propto \frac{1 - (1/2)\pi\sqrt{y}}{T_0} . \tag{14}$$

Equations (12) and (13) illustrate the special features observed in inelastic neutron scattering experiments (see Section 2): the exchange enhancement of dynamic susceptibility leads to a decrease in spin fluctuation energy and an increase in correlation length. Moreover, it is clear that because of equation (13) the correlation length remains moderate even in the event of strong renormalization of dynamic susceptibility.

Raymond et al. [24] and Kambe et al. [48] used the results of self-consistent spin renormalization theory to analyze the spin fluctuations in heavy-fermion compounds. They found that equation (13) provides results that are in good agreement with the experimental data. According to this theory, the rate of decay of nonlocal spin fluctuations, Γ_{IS}, was approximately three times higher than expected, and Kambe et al. [48] attributed this to strong anisotropy. On the whole, spin fluctuation theory provides a good base for analyzing the experimental data. In addition, it shows that intersite spin excitations contribute substantially to the low-temperature thermodynamic characteristics of matter. Thus, the microscopic theory of the strongly correlated state of Fermi systems must incorporate dynamic SRO.

A number of microscopic methods have been developed [57 – 59] to describe SRO in heavy-fermion compounds (metals and insulators). Microscopic equations can be used to derive mean-field equations that allow for SRO [60 – 62]. The following Hamiltonian was used to describe a Kondo lattice:

$$H = E_0 \sum_{i,\sigma} n^{\mathrm{l}}_{i\sigma} + \sum_{\mathbf{k},\sigma} \varepsilon_{\mathbf{k}}\, n^{\mathrm{c}}_{\mathbf{k}\sigma} - J_{\mathrm{K}} \sum_{\langle ij\rangle} \mathbf{S}^{\mathrm{l}}_i \mathbf{S}^{\mathrm{l}}_j - J_{\mathrm{H}} \sum_i \mathbf{S}^{\mathrm{l}}_i \mathbf{S}^{\mathrm{c}}_i\,, \tag{15}$$

where superscripts 'l' and 'c' refer to localized states and to the conduction band, respectively. Both exchange interactions are assumed to be antiferromagnetic: $J_{\mathrm{K}} < 0$ and $J_{\mathrm{H}} < 0$.

The mean-field equations of the paramagnetic phase are obtained by introducing two parameters: one is responsible for the formation of Kondo singlets, $\lambda = \langle 1/2(f^+_i a_i + \mathrm{h.c.})\rangle$, where f^+_j is a localized electron creation operator, and the other is a responsible for correlations between the nearest localized states, $\tau = \langle f^+_{i\sigma} f_{j\sigma}\rangle'$, where the prime means summation over the nearest neighbors. Then the energy of the system can be represented as a function of these parameters [61]:

$$E = 2\sum_{\mathbf{k}} \left[\varepsilon^+_{\mathbf{k}} f(\varepsilon^+_{\mathbf{k}}) + \varepsilon^-_{\mathbf{k}} f(\varepsilon^-_{\mathbf{k}})\right] - zJ_{\mathrm{H}}\,\tau^2 - 2J_{\mathrm{K}}\lambda^2\,, \tag{16}$$

where $\varepsilon^{+\,-}_{\mathbf{k}}$ are two subbands that emerge as a result of hybridization of the itinerant electrons and localized states, and z is the number of nearest neighbors. The ground state is obtained by minimizing the energy in parameters λ and τ. In this variant of the mean-field theory, three different states, determined by two critical temperatures, T_{K} and T_{C}, emerge. At high temperatures the system is in the paramagnetic state with $\lambda = 0$ and $\tau = 0$; at low temperatures ($T < T_{\mathrm{K}}$) and a moderate value of J_{H}, $\tau \neq 0$ and Kondo singlets form in the system, $\lambda \neq 0$; finally, at temperatures higher than T_{K} but lower than T_{C} a state is formed in which there are no Kondo singlets, $\lambda = 0$, but there is SRO between the localized states, $\tau \neq 0$. These results agree qualitatively with the results of numerical calculations [63] by the quantum Monte Carlo method. Note that in the given procedure there is no relationship between renormalization of the quasiparticle band and SRO [62].

3.2 The functional integral method

Kotliar and Ruckenstein [64] have proposed a method for analyzing strongly correlated systems, which uses the functional integral technique. The initial space of Hamiltonian states (8) is extended by introducing auxiliary bosons which are described by creation (annihilation) operators $e^+_i(e_i)$, $p^+_{\sigma i}(p_{i\sigma})$, and $d^+_i(d_i)$. The operators e_i, $p_{i\sigma}$, and d_i act as projection operators on empty, singly filled, and doubly filled states, respectively, of the site i. In terms of the auxiliary bosons, the Hamiltonian (8) is written as follows [64]:

$$\widetilde{H} = \sum_{ij,\sigma} t_{ij}\, a^+_{i\sigma}\, a_{j\sigma}\, z^+_{i\sigma}\, z_{i\sigma} + U\sum_i d^+_i d_i\,, \tag{17}$$

where

$$z_{i\sigma} = (1 - d^+_i d_i - p^+_{i\sigma} p_{i\sigma})^{-1/2} (e^+_i p_{i\sigma} + p^+_{i,-\sigma}\, e_i) \times (1 - e^+_i e_i - p^+_{i,-\sigma} p_{i,-\sigma})^{-1/2}\,.$$

To eliminate nonphysical states, model (17) is augmented with the constraints:

$$a^+_{i\sigma}\, a_{i\sigma} = p^+_{i\sigma}\, p_{i\sigma} + d^+_i\, d_i\,,$$

$$\sum_\sigma p^+_{i\sigma}\, p_{i\sigma} + e^+_i\, e_i + d^+_i\, d_i = 1\,. \tag{18}$$

The effective action corresponding to the Hamiltonian (17) contains (time-independent) Lagrange multipliers that ensure that the conditions (18) are met. The free energy of the system (17) can be calculated in the paramagnetic saddle-point approximation. It was found that such an approximation corresponds to the Gutzwiller approximation [15] (see also Section 3.3), i.e., there are no correlations between the nearest neighbors. To allow for nonlocal correlations, Trapper et al. [65] introduced two Bose fields, $\widetilde{m}$ and $\widetilde{\xi}$, into the scheme. The local magnetization and the internal magnetic field that fluctuate in time were expressed in terms of these fields as $m_i = \pm\widetilde{m}$ and $\xi_i = \pm\widetilde{\xi}$, where the sign depends on the index i. Next, using the paramagnetic saddle point as the zeroth approximation, Trapper et al. [65] did a perturbation-theory expansion. Then a new solution of the saddle-point type was calculated, but this was already over all Bose fields, including $\widetilde{m}$ and $\widetilde{\xi}$. Figure 7 shows the results of calculations of the phase diagram of the Hubbard model on a square lattice for three phases: paramagnetic [64], paramagnetic with SRO [65], and antiferromagnetic. Clearly, at large values of U/t SRO develops in the system; the paramagnetic phase with SRO encompasses a substantial part of the phase diagram. Although at exact half band-filling this state is masked by long-range AFM order, it has a lower energy than the paramagnetic phase. Note that the absence of magnetic correlations in the PM phase is an incorrect result for finite-dimensional lattices. Even at $U = 0$, due to the Pauli exclusion principle there are nonlocal correlations of the exchange-hole type between fermions with the same spin. When Coulomb interaction is included, these correlations become stronger. Hence, the first-order PM – PM-SRO transition obtained by Trapper et al. [65] may be a consequence of this drawback of the method.

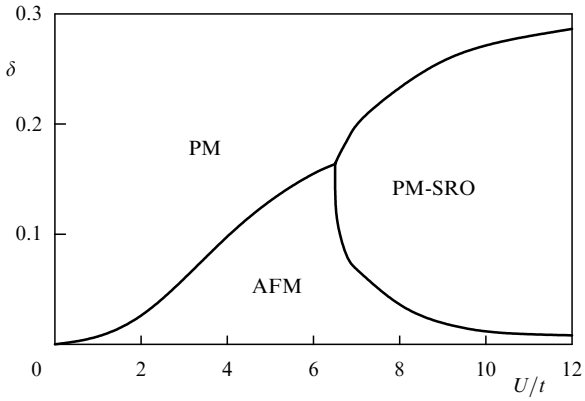

Figure 7. Phase diagram of the Hubbard model on a two-dimensional lattice (the auxiliary boson method) [65]. AFM stands for the antiferromagnetic phase, PM for the paramagnetic phase without correlations, and PM-SRO for the paramagnetic phase with short-range order. The number of electrons per lattice site is $1 - \delta$.

3.3 Gutzwiller's method, $1/D$ expansion, and the variational Monte Carlo method

The Gutzwiller trial variational function [15, 14, 66, 67] and its modifications [59, 68] probably constitute the most popular variational approach to the problem of a strongly correlated state. The Gutzwiller trial wave function can be written in the form [67]

$$|\psi\rangle = g_0^{\hat{X}}|\varphi_0\rangle\,, \tag{19}$$

where $\widehat{X} = \sum_i n_{i\uparrow}\, n_{i\downarrow}$, g_0 is a real parameter whose value is in the interval [0, 1] for $U > 0$, and $|\varphi_0\rangle$ is the initial N-particle wave function of uncorrelated electrons; e.g., for a crystal this function can be built using Bloch functions:

$$\prod_{\mathbf{k}<\mathbf{k}_{\mathrm{F}\uparrow}} a^{+}_{\mathbf{k}\uparrow} \prod_{\mathbf{k}<\mathbf{k}_{\mathrm{F}\downarrow}} a^{+}_{\mathbf{k}\downarrow}|0\rangle\,, \tag{20}$$

where $\mathbf{k}$ is the fermion wave vector, and $\mathbf{k}_{\mathrm{F}\sigma}$ is the Fermi wave vector for fermions with spin σ. The number of particles comprising the system is assumed to be large but finite. There are also other equivalent representations of the trial wave function (19). For instance, the operator on the right-hand side of (19) can be written in the form

$$g_0^{\hat{X}} = \prod_i \left[1 - (1 - g_0)\, n_{i\uparrow}\, n_{i\downarrow}\right] \tag{21}$$

or

$$g_0^{2\hat{X}} = \prod_i \left[1 - (g_0^2 - 1)\, n_{i\uparrow}\, n_{i\downarrow}\right]. \tag{22}$$

The expressions (21) and (22) are often used in diagrammatic expansions [17–19, 70].

To clarify the meaning of the trial function (19), let us expand $|\varphi_0\rangle$ in the configurations [15]:

$$|\varphi_0\rangle = \sum_{\Gamma} A_{\Gamma}|\Gamma\rangle\,, \tag{23}$$

where $|\Gamma\rangle$ is the vector of a state in the configuration space, i.e., this is a state of the form $a^{+}_{i_1\sigma_1} a^{+}_{i_2\sigma_2} \ldots a^{+}_{i_{\mathrm{N}}\sigma_{\mathrm{N}}}|0\rangle$, where the indices i and σ denote the number of the lattice site and the spin for each electron, with the set of indices $\{i_1, i_2, \ldots, i_{\mathrm{N}}, \sigma_1, \sigma_2, \ldots, \sigma_{\mathrm{N}}\}$ determining the given configuration Γ, and A_{Γ} is the complex-valued amplitude of the configuration $|\Gamma\rangle$. The relative phases between different configurations reflect the different symmetries of the system (the antisymmetric nature of the wave function under particle permutations, the point symmetry, the translational symmetry of the crystal, etc.) [15]. Clearly, the operator $g_0^{\hat{X}}$ is invariant under particle permutations, transformations of the point group, and translations. Thus, the trial wave function (19) retains all the symmetries of the initial wave function. Here, thanks to the factor g_0^D, the greater the number of doubly occupied sites in the given configuration (D) the greater a decrease in the amplitude of each configuration.

Next, we can calculate the energy of the Hubbard Hamiltonian (8) on the trial wave function (19):

$$E = \frac{\langle\psi|H|\psi\rangle}{\langle\psi|\psi\rangle}\,. \tag{24}$$

Here Gutzwiller made [15] a strong assumption which became known as the Gutzwiller approximation. The essence of this approximation is that the states of two different sites are assumed to be independent. This reduces the problem of determining the system energy to a purely combinatorial problem. The parameter g_0 can be expressed in terms of $x = \langle n_{i\uparrow}\, n_{i\downarrow}\rangle$ and excluded from Eqn (24). As a result we get [67]

$$E = \sum_{\sigma} q_{\sigma}\bar{\varepsilon}_{\sigma} + xU\,, \tag{25}$$

where

$$q_{\sigma} = \frac{\left\{\left[(n_{\sigma} - x)(1 - n_{\sigma} - n_{-\sigma} + x)\right]^{1/2} + \left[x(n_{-\sigma} + x)\right]^{1/2}\right\}^2}{n_{\sigma}(1 - n_{\sigma})}\,, \tag{26}$$

with $n_{\sigma} = \langle n_{i\sigma}\rangle$, and $\bar{\varepsilon}_{\sigma}^{0} = \sum_{\mathbf{k}<\mathbf{k}_{\mathrm{F}}} \varepsilon^{0}_{\mathbf{k}\sigma}$ is the average kinetic energy of electrons with spin σ. Now, to find the ground-state energy of the system, the energy E is minimized with respect to the parameter x. As U increases, the parameter q_{σ} decreases. Such behavior can be shown [27] to correspond to the narrowing of the quasiparticle band and to an increase in the effective quasiparticle mass $q_{\sigma} = m_{\mathrm{eff}}^{-1}$.

As noted earlier, nonlocal dynamical configurations disappear in the limit of an infinite-dimensional lattice, with the result that in this case the Gutzwiller trial wave function, together with the Gutzwiller approximation, produces very good results. But the Gutzwiller approximation is too strong in the case of a finite-dimensional lattice, since it completely excludes nonlocal correlations between the particles. For instance, it is a well-known fact that the metal–insulator phase transition that emerges in the PM phase with half band-filling at the critical value $U_{\mathrm{C}} = 8|\bar{\varepsilon}_0|$, where $\bar{\varepsilon}_0 = \bar{\varepsilon}_{\uparrow}^{0} + \bar{\varepsilon}_{\downarrow}^{0}$, exists only in the limit of an infinite-dimensional lattice [9].

Calculations of the ground-state energy for the Gutzwiller trial wave function on finite-dimensional lattices are much more complicated if one does not use the Gutzwiller approximation. Metzner and Vollhardt [17–19] proposed a diagrammatic expansion of the operator (22) in powers of the parameter $(g_0^2 - 1)$. The lines in the diagrams corresponded to a one-particle density matrix of the noninteracting system, $\langle\varphi_0|a^{+}_{i\sigma}a_{j\sigma}|\varphi_0\rangle$, while the vertices corresponded to the parameter $(g_0^2 - 1)$. Using this expansion, Metzner and Vollhardt [17] and Gebhard and Vollhardt [69] were able to obtain an exact solution for the case of a one-dimensional chain. For the reason we have just discussed, the diagrammatic expansion is much simpler in the case of an infinite-dimensional lattice. The most complicated cases are still those of two- and three-dimensional systems. The situation becomes somewhat simpler if the Hartree–Fock solution for a given U is chosen as the initial wave function. To this end a new parameter x_i which depends on the number of the site, is introduced instead of $g^2 - 1$ and a new operator $\widehat{K} = \sum_i [n_{i\uparrow}\, n_{i\downarrow} - (n_{i\uparrow}\, n_{i\downarrow})_{\mathrm{HF}}]$ is introduced instead of $\widehat{X}$, where $(n_{i\uparrow}\, n_{i\downarrow})_{\mathrm{HF}} = \langle n_{i\uparrow}\rangle n_{i\downarrow} + n_{i\uparrow}\langle n_{i\downarrow}\rangle - \langle n_{i\uparrow}\rangle\langle n_{i\downarrow}\rangle$ is the 'Hartree–Fock' value of the operator $n_{i\uparrow}\, n_{i\downarrow}$. This is followed by a diagrammatic expansion of the operator $g_0^{2\widehat{K}} = \prod_i \{1 + x_i[n_{i\uparrow}\, n_{i\downarrow} - (n_{i\uparrow}\, n_{i\downarrow})_{\mathrm{HF}}]\}$, which is called the expansion in terms of powers of $1/D$ [70]. Calculations of the ground-state energy for the Gutzwiller trial wave function that use the expansion to $1/D^2$ order lead to results that are very close to those of the Gutzwiller approximation. There emerges a metal–insulator phase transition (nonphysical for finite-dimensional lattices) at U_{C} that differs from the critical value in the Gutzwiller approx-

imation only by 4% for a three-dimensional cubic lattice and by 8% for a two-dimensional square lattice [70].

Two questions arise when one analyzes the results of the $1/D + 1/D^2$ expansion. First, it is unclear how rapidly the series converges and hence what the accuracy of the ground-state energy calculations is. Second, the Gutzwiller trial wave function contains a variational parameter responsible only for intrasite correlations, which is sufficient for an infinite-dimensional lattice. However, it is not obvious that this parameter provides an adequate description of strongly correlated states on two- and three-dimensional lattices.

The answer to the first question follows from the results of a numerical calculation of the ground state of the Gutzwiller trial wave function on finite-dimensional lattices. The calculations were carried out for finite clusters by the variational Monte Carlo method [20] without the Gutzwiller approximation. The crystal's ground-state energy was determined by extrapolating the dependence of the cluster's ground-state energy on the cluster size to an infinite cluster. The results of calculations for the PM and AFM phases at half band-filling are shown in Figs 8 and 9. These calculations

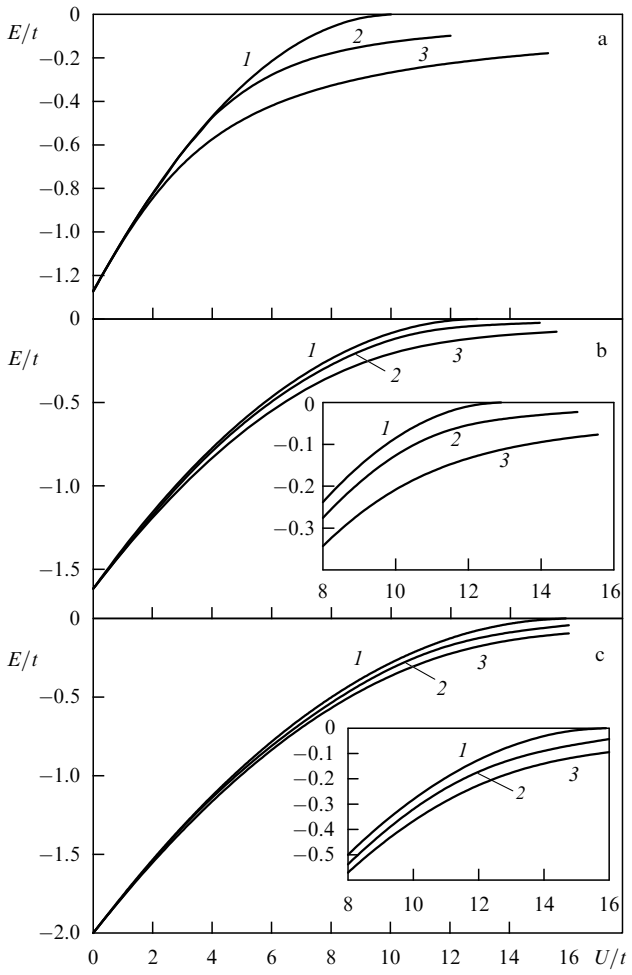

Figure 8. Ground-state energy of fermions in the PM phase for (a) a one-dimensional chain: *1* — Gutzwiller's solution [15], *2* — variational theory of SRO [22] [minimization of Eqn (55)], and *3* — exact solution [13] (AFM phase); (b) a two-dimensional square lattice and (c) a simple cubic lattice: *1* — Gutzwiller's solution, *2* — variational Monte Carlo method [20], and *3* — variational theory of SRO [22] [minimization of Eqn (55)]. The insets show enlarged fragments of the diagrams near U_C.

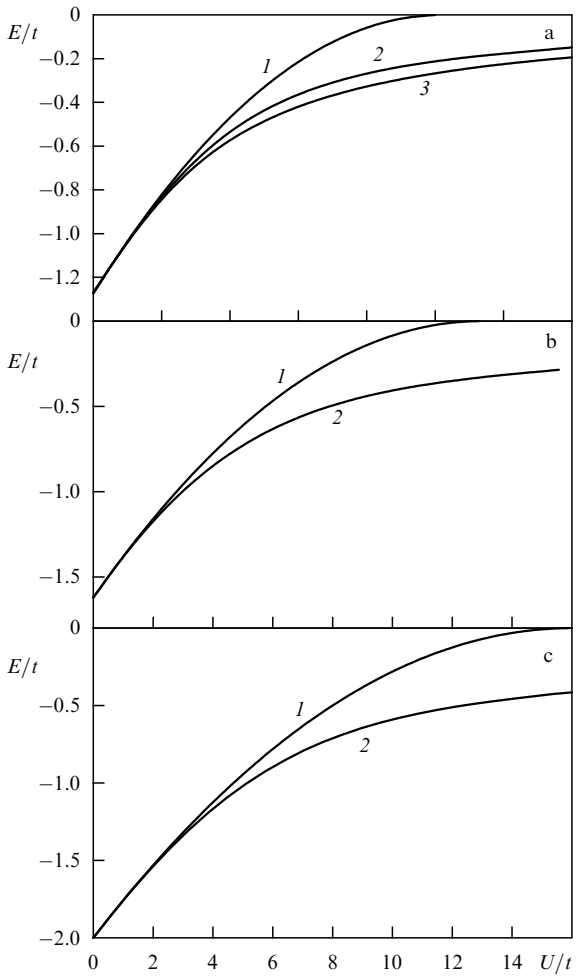

Figure 9. Ground-state energy of fermions in the AFM phase for (a) a one-dimensional chain: *1* — Gutzwiller's solution [15], *2* — variational theory of SRO [22], and *3* — the exact solution [13]; (b) a two-dimensional square lattice and (c) a simple cubic lattice: *1* — Gutzwiller's solution and *2* — variational theory of SRO [22].

show that there is no phase transition near U_C. Thus, at least for $U \geqslant U_C$ the $1/D + 1/D^2$ expansion is incorrect.

To get an answer to the second question, let us examine the limit $U \gg \Delta$, were Δ is the width of the initial band. In this limit, the well-known $t-J$ model [71 – 74] is appropriate:

$$H = -t \sum_{ij\sigma} (1 - n_{i,-\sigma}) a^{+}_{i\sigma} a_{j\sigma} (1 - n_{i,-\sigma}) + J \sum_{ij} \left(\mathbf{S}_i \mathbf{S}_j - \frac{1}{4} n_i n_j \right), \quad (27)$$

where $\mathbf{S}_i$ is the spin operator, and $J = 2t^2/U$. Doubly occupied states of the lattice sites are excluded from the state space of the $t-J$ model. Now we turn to the Gutzwiller trial wave function on a finite-dimensional lattice in this limit. It is a well-known fact (see Ref. [74]) that the $t-J$ model contains nonlocal spin correlations, i.e., $\langle S_{zi} S_{zj} \rangle' \neq 0$, where S_{zi} is the spin projection on the z axis, and the prime indicates nearest-neighbor averages. Since doubly occupied states have been excluded, the variational parameter in the trial function is fixed ($g_0 = 0$). Thus, for the Gutzwiller trial wave function the quantity $\langle S_{zi} S_{zj} \rangle'$ in the $t-J$ model is a constant. On the other hand, the Hamiltonian contains two constants, t and J. Their

ratio determines the amplitude of short-range correlations. Clearly, the Gutzwiller function cannot by itself correctly describe short-range correlations on a finite-dimensional lattice (even outside the scope of the Gutzwiller approximation). The same is true of the dynamical mean-field theory (DMFT). Thus, a variational investigation of short-range correlations requires the introduction of additional variational parameters responsible for short-range correlations.

4. Variational theory of SRO

4.1 General properties of the trial wave function

Let us now study the properties of a trial wave function that explicitly contains SRO. In the most general form this function can be written as follows [21, 22]:

$$|\psi\rangle = \widetilde{F}|\varphi_0\rangle = \prod_\lambda g_\lambda^{\hat{P}_\lambda}|\varphi_0\rangle\,, \tag{28}$$

where, in addition to the Gutzwiller multiplier, the product contains a set of projection operators $\widehat{P}_\lambda$ on all possible configurations of the state of a lattice site and a pair of sites that are the nearest neighbors. The real-valued parameter g_i may vary in the interval $[0, \infty)$, which makes it possible to increase or decrease the amplitudes of the different configurations of the pair of sites.

For example, let us determine the explicit form of the trial wave function for the PM phase of a nondegenerate half-filled band. Here there are four projection operators, each isolating a definite state of the lattice sites,

$$\begin{aligned}
\widehat{X}_1 &= \sum_i (1-n_{i\uparrow})(1-n_{i\downarrow})\,,\\
\widehat{X}_2 &= \sum_i n_{i\uparrow}(1-n_{i\downarrow})\,,\\
\widehat{X}_3 &= \sum_i (1-n_{i\uparrow})n_{i\downarrow}\,,\\
\widehat{X}_4 &= \sum_i n_{i\uparrow}\,n_{i\downarrow}\,,
\end{aligned} \tag{29}$$

and 10 projection operators on the states of nearest-neighbor site pairs of the following form:

$$\begin{aligned}
\widehat{Y}_1 &= \sum_{\langle ij\rangle} (1-n_{i\uparrow})(1-n_{i\downarrow})(1-n_{j\uparrow})(1-n_{j\downarrow})\,,\\
\widehat{Y}_2 &= \sum_{\langle ij\rangle} n_{i\uparrow}\,n_{i\downarrow}\,n_{j\uparrow}\,n_{j\downarrow}\,,
\end{aligned} \tag{30}$$

etc. (Table 2).

Table 2. Configurations of a nearest-neighbor pair in the Hubbard model (PM phase, half band-filling).

Operator	Configuration		Degeneracy multiplicity
	Site i	Site j	
$\widehat{Y}_1$			1
$\widehat{Y}_2$	$\uparrow\downarrow$	$\uparrow\downarrow$	1
$\widehat{Y}_3$	$\uparrow\downarrow$		2
$\widehat{Y}_4$	$\uparrow$		2
$\widehat{Y}_5$	$\downarrow$		2
$\widehat{Y}_6$	$\uparrow$	$\uparrow$	1
$\widehat{Y}_7$	$\uparrow$	$\downarrow$	2
$\widehat{Y}_8$	$\uparrow\downarrow$	$\uparrow$	2
$\widehat{Y}_9$	$\uparrow\downarrow$	$\downarrow$	2
$\widehat{Y}_{10}$	$\downarrow$	$\downarrow$	1

Next, we limit ourselves to lattices in which the total number of nearest-neighbor pairs is $zL/2$, where z is the number of the nearest neighbors of a site, and L is the total number of lattice sites. We define the normalized eigenvalues of the operators (29) and (30) as follows:

$$x_\lambda|\Gamma\rangle = L^{-1}\widehat{X}_\lambda\,|\Gamma\rangle\,, \qquad y_\lambda|\Gamma\rangle = \left(\frac{zL}{2}\right)^{-1}\widehat{Y}_\lambda|\Gamma\rangle\,. \tag{31}$$

Clearly, the configurations $|\Gamma\rangle$ are the eigenvectors of these operators. Then the eigenvalues prove to be related by the normalization conditions [1, 21, 22]

$$\sum_\lambda x_\lambda = 1\,, \qquad \sum_\lambda \beta_\lambda y_\lambda = 1\,, \tag{32}$$

where β_λ is the degeneracy multiplicity, and by the self-consistency conditions

$$\begin{aligned}
&y_1 + y_3 + y_4 + y_5 = x_1\,,\\
&y_2 + y_3 + y_8 + y_9 = x_4\,,\\
&y_4 + y_6 + y_7 + y_8 = x_2\,,\\
&y_5 + y_7 + y_9 + y_{10} = x_3\,.
\end{aligned} \tag{33}$$

Since the concentrations of fermions of each spin are assumed to be fixed, there is only one independent parameter x_λ, as there is in the Gutzwiller approximation. There are also seven independent parameters y_λ. In the case of half band-filling, for the PM phase (total spin zero) there are additional conditions [21, 22]:

$$y_1 = y_2\,, \qquad y_6 = y_{10}\,, \qquad y_4 = y_5 = y_8 = y_9\,. \tag{34}$$

After the additional conditions (34) are introduced, the number of the independent parameters y_λ drops to three. Let us take $x = x_1 = x_4$, y_3, y_4, and y_7 as the independent parameters. Next, taking into account the additional degeneracy that emerges because of the conditions (34), we arrive at the final form of the trial wave function of the PM phase at half filling:

$$|\psi\rangle = g_0^{\hat{X}}\, g_3^{\beta_3\hat{Y}^3}\, g_4^{4\beta_4\hat{Y}^4}\, g_7^{\beta_7\hat{Y}_7}|\varphi_0\rangle = \widehat{F}|\varphi_0\rangle\,. \tag{35}$$

Now let us discuss the main properties of the trial wave function (28). The Gutzwiller trial wave function (19) and the trial wave function (35) are particular cases of Eqn (28), with the result that all the formal properties listed in the next paragraph are also true. First, we must select a many-particle initial wave function $|\varphi_0\rangle$. It must be antisymmetric under particle permutations and invariant with respect to certain symmetry transformations. For molecules this is the point symmetry group, while for a crystal structure the translation group is added. The operator $\widehat{F}$ on the right-hand side of Eqn (19) is a polynomial in $n_{i\sigma}$, so that the trial wave function remains antisymmetric under particle permutations. This operator must be invariant under the same transformations as the initial wave function (point and translational transformations). Then all the symmetries are passed from the initial wave function to the trial wave function. In the sections that follow we will discuss specific examples of the selection of the trial wave function.

Here are some of the formal properties of the operators $\widehat{F}(g_0, \ldots, g_\Lambda)$. Note that the operators $g_\lambda^{\hat{P}_\lambda}$ commute with each other. The set of operators $\widehat{F}(g_0, \ldots, g_\Lambda)$ has (provided

that $g_i \neq 0$) the following properties: $\widehat{F}(g_0,\ldots,g_\Lambda)\times \widehat{F}(g'_0,\ldots,g'_\Lambda)=\widehat{F}(g''_0,\ldots,g''_\Lambda)$, where $g''_i = g_i g'_i$. Furthermore, there is an identity operator ($g_i = 1$) and an inverse of any operator: $\widehat{F}^{-1}(g_0,\ldots,g_\Lambda) = \widehat{F}(1/g_0,\ldots,1/g_\Lambda)$. Thus, the operators $\widehat{F}(g_0,\ldots,g_\Lambda)$ comprise a group. At $g_i = 0$ the operator $\widehat{F}(g_0,\ldots,g_\Lambda)$ is not a member of a group since it has no inverse operator. Another important property is that $\widehat{F}(g_0,\ldots,g_\Lambda)$ is nonunitary.

4.2 Electron correlations in molecules and clusters

Many-particle correlations appear in all many-electron systems with a strong interaction: atoms, molecules, and crystalline solids. Actually, it is easy to write the trial wave function of type (19) for any system. What is difficult is to calculate the ground-state energy. There is a distinct difference between the theoretical methods used in solving the problem of correlations in quantum chemistry (atoms, small molecules, and clusters) and those used in solid state physics (crystalline systems) [75]. In this section we discuss the quantum-chemical approach.

We begin by estimating the dimensionality of the Hilbert space of states for a small molecule. For instance, for the CH_4 molecule the minimum set of basis functions of the molecule is formed by 1S, 2S, and three 2P atomic orbitals of carbon and four 1S orbitals of hydrogen. Then the total number of singlet states of the molecule, with allowance for the restrictions imposed by the symmetry of the molecule, is 5292, that of triplet states is 7560, etc. [68]. If extended sets of basis functions are used, these numbers get much bigger. For instance, the use of a set of the (DZ + P) type, consisting of 35 basis functions for the same molecule, results in approximately 2×10^{11} singlet states. Thus, a direct numerical calculation of the ground state with allowance for all states is possible only for small molecules of the H_2O type with a minimum basis [68]. On the other hand, it is obvious that different vectors enter the ground state with different weights, whereby the initial space of states can be restricted by excluding configurations whose probabilities are very low. Let us assume that for a molecule, we know a solution of the Hartree – Fock type, i.e., the ground state (we assume that this is the initial state $|\varphi_0\rangle$) and the corresponding set of molecular orbitals. It is convenient to split the Hamiltonian of the problem into two parts [75]: $H = H_{\rm HF} + H_{\rm r}$, where the first term on the right-hand side is the diagonal part in the representation of Hartree – Fock molecular orbitals, and the second is the remaining part of the Hamiltonian. Allowance for correlations leads to inclusion into the ground state of vectors of the type $a^+_{i\sigma}a_{i\sigma}|\varphi_0\rangle$, $a^+_{i\sigma}a^+_{j\sigma'}a_{j\sigma'}a_{i\sigma}|\varphi_0\rangle$, etc., where $a^+_{i\sigma}$ is the electron creation operator on the ith molecular orbital. Intuitively, it is clear that the highly excited states of a small molecule with a large number of electron – hole pairs have a high energy and must have a relatively small weight, whereby they can be excluded from the state space.

This idea has been realized in many ways for atoms, molecules, and clusters [68, 75 – 78]. The most powerful (and the most complicated) approach here is probably the use of the cumulant representation [68, 79]. Below we follow Ref. [75], where Horsch and Fulde proposed a simple, clear formalism of expanding the operator $\widehat{F}$ in powers of the operators $\widehat{X}$ and $\widehat{Y}$. We write the trial wave function (28) in the form

$$|\psi\rangle = \exp(\widehat{G})|\varphi_0\rangle = \exp\Big(-\sum_{ij}\eta_{i\sigma j\sigma'}\,n_{\sigma i}\,n_{j\sigma'}\Big)|\varphi_0\rangle\,. \quad (36)$$

Clearly, the parameters $\eta_{i\sigma j\sigma'}$ stand for $\ln g_\lambda$ from equation (28). If in the operator expansion of the exponential we keep only the first term, we arrive at a simple ansatz for calculating the correlation energy of a molecule [80]:

$$|\psi\rangle = \Big(1 - \sum_{ij}\eta_{i\sigma j\sigma'}\,n_{\sigma i}\,n_{j\sigma'}\Big)|\varphi_0\rangle\,. \quad (37)$$

It occurs that for small molecules even the ansatz (37) provides a fairly accurate value of the correlation energy of the ground state (usually about 97% of the exact value) [68, 77, 80]. Using the coupled-clusters theorem, one can develop a diagrammatic technique for calculating the ground-state energy with the trial wave function (36). The expression for the ground-state energy has the form

$$E=\frac{\langle\varphi_0|\exp(\widehat{G})H\exp(\widehat{G})|\varphi_0\rangle}{\langle\varphi_0|\exp(\widehat{G})\exp(\widehat{G})|\varphi_0\rangle}=\frac{\langle\exp(\widehat{G})H\exp(\widehat{G})\rangle}{\langle\exp(\widehat{G})\exp(\widehat{G})\rangle}\,. \quad (38)$$

The exponentials in the numerator of Eqn (38) must be expanded in a series. The Wick theorem makes it possible to express arbitrary products of the $\widehat{G}^nH\widehat{G}^m$ type in terms of pair averages of operators of electron creation and annihilation in the ith state. Each term in the expansion can be expressed by a diagram which can be either connected or disconnected. After certain transformations are done, the numerator in Eqn (38) becomes factorized as follows:

$$\big\langle\exp(\widehat{G})H\exp(\widehat{G})\big\rangle = \sum_{q,k}\frac{1}{q!(k-q)!}\,\big\langle\widehat{G}^qH\widehat{G}^{k-q}\big\rangle_C \times\sum_{m,n}\frac{1}{(m-q)!(n-k+q)!}\,\big\langle\widehat{G}^{m-q}\widehat{G}^{n-k+q}\big\rangle\,, \quad (39)$$

where $\langle\ldots\rangle_C$ means that the structure is completely connected, and the second factor is simply the expansion of the numerator and is canceled out. Thus, we arrive at the final result [75]

$$E = \big\langle\exp(\widehat{G})H\exp(\widehat{G})\big\rangle_C\,, \quad (40)$$

i.e., the ground state is determined solely by connected diagrams. Note that in deriving Eqn (40) no assumptions concerning the structure of $\widehat{G}$ and H were made.

Extensive studies of correlations in small molecules have been conducted (see Ref. [68]). Ordinarily, the complete set of parameters is not used in calculations — the common practice is to use two of these parameters, the one corresponding to spin correlations ($\eta'_{ij}\mathbf{S}_i\mathbf{S}_j$) and the one corresponding to density correlations ($\eta''_{ij}n_in_j$). Useful approximate algebraic expressions for the correlation energy were obtained within the local ansatz (37). For instance, for various double bonds in organic substances [68, 81] these expressions are

$$\begin{aligned}
E_{\rm corr}(\mathrm{C-H}) &= -0.44 - 5.9\times10^{-3}(d-1.08)\,,\\
E_{\rm corr}(\mathrm{C-C},\sigma) &= -0.27 - 3.0\times10^{-3}(d-1.3)\\
&\quad - 1.0\times10^{-4}(d-1.3)^2\,,\\
E_{\rm corr}(\mathrm{C-C},\pi) &= -1.57 - 3.47\times10^{-2}(d-1.3)\\
&\quad - 6.28\times10^{-4}(d-1.3)^2\,.
\end{aligned} \quad (41)$$

Here the energy is expressed in electronvolts and the bond length d in angstroms, and σ and π denote the type of

carbon–carbon bond. Comparison with the experimental values of the correlation energy shows that the accuracy of the formulas (41) for small organic molecules is good.

4.3 Ground state of strongly correlated electron systems on a lattice in the Hubbard model

The use of quantum chemistry methods in solving the problem of SRO in crystalline systems proved not to be very productive. A crystalline system contains a very large number of electrons, with the result that the eigenvalues of the operators P_λ are large numbers. This means that in the expansion of the exponential in Eqn (36) we cannot limit ourselves only to the first terms. One is able to sum only diagrams of a certain class and arrive at a solution of the RPA type [75]. This is clearly insufficient for a microscopic analysis of SRO. The variational cluster method (VCM), or the Kikuchi pseudoensemble method, makes it possible to calculate averages on the trial wave function (28) without resorting to expansion (36) [82–85]. This method is widely used in calculations of the ground state and thermodynamic properties of magnetic substances [1, 82, 83, 86] and disordered systems [87, 88], kinetic phenomena [89, 90], etc. Its modern rigorous formulation is based on a description in terms of cumulants [91, 92]. Below we follow the well-established clear formulation in terms of the variational cluster method [1, 82, 83].

We begin by calculating the ground-state energy in the Hubbard model in the PM phase with half band-filling, i.e., for the trial wave function (35). It is convenient to do all calculations using the equiprobable state $|\varphi_{ep}\rangle$ in which the absolute value of the amplitude is the same for all configurations, or $|A_\Gamma| = \text{const}$. Note that this state is not the initial state $|\varphi_0\rangle$, since even in the case of noninteracting fermions in the ground state (20) there are nonlocal correlations. First we calculate the function $|\varphi_0\rangle$ according to the variational procedure $|\varphi_0\rangle = \widehat{F}|\varphi_{ep}\rangle$, assuming that $U = 0$. Then we find the wave function of the correlated system as $|\psi\rangle = \widehat{F}'|\varphi_{ep}\rangle$. The group properties of the operator $\widehat{F}$ suggest that we have found the sought after transformation of the initial wave function into the correlated wave function:

$$|\psi\rangle = \widehat{F}'\widehat{F}^{-1}|\varphi_0\rangle\,. \tag{42}$$

Let us now find the norm of an arbitrary trial wave function of the type $|\psi\rangle = F|\varphi_{ep}\rangle$. Following Refs [21, 22], we write the norm as follows:

$$\begin{aligned}\langle\psi|\psi\rangle &= \sum_{\{x,y_3,y_4,y_7\}} W_{\{x,y_3,y_4,y_7\}}\, g_0^{2Lx}\, g_3^{2zLy_3}\, g_4^{8zLy_4}\, g_7^{2zLy_7}\\ &= \sum_{\{x,y_3,y_4,y_7\}} R_{\{x,y_3,y_4,y_7\}}\,.\end{aligned} \tag{43}$$

Summation in Eqn (43) is over all sets $\{x, y_3, y_4, y_7\}$. There can be several configurations corresponding to a single set of independent variables. Here $W_{\{x,y_3,y_4,y_7\}}$ is the number of configurations [1] corresponding to the fixed set $\{x, y_3, y_4, y_7\}$. We call this quantity the weight of the set, and to calculate it we employ the following method. We calculate the number of ways in which 10 possible configurations of a pair of sites (see Table 2) can be arranged among the $zL/2$ bonds linking the nearest neighbors. As a result we obtain

$$Q = \frac{(zL/2)!}{\prod_\lambda \left[(zy_\lambda L/2)!\right]^{\beta_\lambda}}\,. \tag{44}$$

Here, for the sake of simplicity we have discarded the lower indices. This quantity gives us an estimate of W that is greatly overvalued, since there appear many false configurations in which different states correspond to the same site (Fig. 10). Now we can estimate the fraction of 'correct' distributions in the configuration pseudoensemble. We arrange the possible states of site $\widehat{X}_\lambda$ among the zL sites of the pseudolattice. In a correct configuration the state of each site is uniquely defined. Then the fraction of correct configurations in pseudoensemble is

$$\Gamma = \frac{L!\prod_\lambda (x_\lambda zL)!}{(zL)!\prod_\lambda (x_\lambda L)!}\,. \tag{45}$$

Finally, the Kikuchi hypothesis states that

$$W = \Gamma Q\,. \tag{46}$$

Note that this hypothesis proves to be exact for Bethe lattices [1, 84]. For lattices that have closed paths it leads to an approximate solution. Below we discuss ways of incorporating closed paths into the calculation scheme. The dependent parameters x_λ and y_λ in Eqns (44) and (45) are expressed in terms of the independent parameters as follows:

$$\begin{aligned} x_2 &= x_3 = \frac{1}{2} - x\,,\\ y_1 &= y_2 = x - y_3 - 2y_4\,,\\ y_6 &= y_{10} = \frac{1}{2} - x - y_7 - 2y_4\,. \end{aligned} \tag{47}$$

In the thermodynamic limit $L \to \infty$, as usual [1, 15, 66, 82], we can limit ourselves to summing only those terms in the series that are close to the maximum term, i.e., for which the condition $\{x, y_3, y_4, y_7\} \to \{x, y_3, y_4, y_7\}_{\max}$ is met. The remaining terms in the series prove to be exponentially small. Since the function R is positive, it is convenient to look for the maximum of its logarithm instead of the function proper. Let us transform all the factorials in R by using Stirling's formula. Then we find the logarithm of the expression and retain the leading terms in L. Such a procedure can be shown to be equivalent to the substitution $(zL/2)! \to (L!)^{z/2}$ used in Refs [1, 82, 83]. Direct calculations

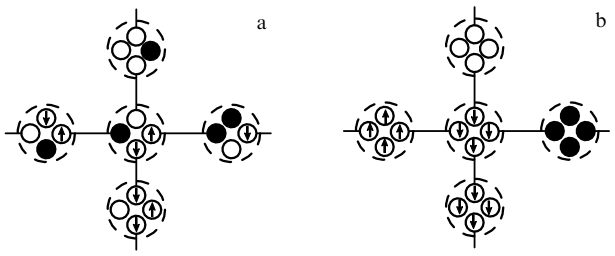

Figure 10. Arrangement of pair configurations in the variational cluster method among the lattice bonds: (a) 'incorrect' configuration, and (b) 'correct' configuration.

[1] To within a constant factor, which is unessential for further calculations.

yield

$$L^{-1}\ln W = 2(z-1)\left[x\ln x + \left(\frac{1}{2}-x\right)\ln\left(\frac{1}{2}-x\right)\right] - z(y_2\ln y_2 + y_3\ln y_3 + 4y_4\ln y_4 + y_6\ln y_6 + y_7\ln y_7)\,, \quad (48)$$

where y_2 and y_6 are given in Eqn (47). The domain of the function $L^{-1}\ln R$ is limited by the conditions (33) and (47) and the requirement that x_λ and y_λ be positive. For finite parameters g_i the gradient of this function at the boundaries is directed inside this domain, with the result that the global maximum of the function $L^{-1}\ln R$ is its internal maximum. In this case the equations $\partial(\ln R)/\partial\eta_\lambda = 0$ are the necessary conditions for a maximum, with $\eta_\lambda = x, y_3, y_4, y_7$. Using these equations, we can express the parameters g_i in terms of x, y_3, y_4, and y_7 as follows:

$$g_0 = \left(\frac{1/2-x}{x}\right)^{z-1}\left(\frac{x-y_3-2y_4}{1/2-x-y_7-2y_4}\right)^{z/2},$$
$$g_3^2 = \frac{y_3}{x-y_3-2y_4}\,, \quad (49)$$
$$g_4^4 = \frac{4y_4^2}{(1/2-x-y_7-2y_4)(x-y_3-2y_4)}\,,$$
$$g_7^2 = \frac{y_7}{1/2-x-y_7-2y_4}\,.$$

Note that $L^{-1}\ln R$ is a strictly convex function in the variables y_3, y_4, and y_7 for a fixed x. This means that actually we are looking for a maximum of a function of an implicitly defined variable rather than a function of four variables.

To calculate the ground-state energy of the Hamiltonian (8), we must find the first-order density matrix on the trial function (35):

$$\rho_1 = L^{-1}\frac{\langle\psi|\sum_{\langle ij\rangle,\sigma}(a_{i\sigma}^{+}a_{j\sigma} + \text{h.c.})|\psi\rangle}{\langle\psi|\psi\rangle}\,. \quad (50)$$

Here one encounters a substantial complication in comparison to Gutzwiller's method, since the hopping of a fermion from site i to site j changes not only the configuration of the i–j pair but also the configurations of the adjacent site pairs i–k and j–l in the lattice (Fig. 11a). Let us fix a certain configuration of a lattice fragment consisting of the i–j bond and the adjacent bonds (Fig. 11a) and let us calculate the function W for the remaining lattice by equations (44)–(46). Then the fraction of configurations containing this fragment can be written in the following form:

$$\frac{W'}{W} = y_{(ij)}\prod_k\left(\frac{y_{(ki)}}{x_{(i)}}\right)\prod_l\left(\frac{y_{(jl)}}{x_{(j)}}\right), \quad (51)$$

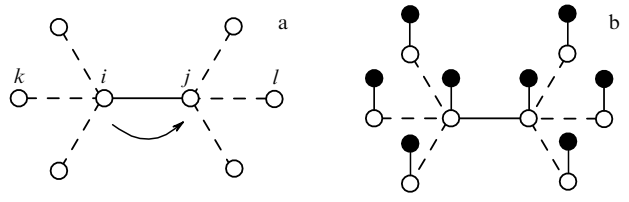

Figure 11. (a) Fragment of a lattice with $z = 4$. When a fermion hops from site i to site j, the configurations of the adjacent pairs change, too. (b) Fragment of the equivalent Kondo–Hubbard lattice; solid circles denote localized states.

where by $y_{(\alpha\beta)}$ we mean the value of y_λ corresponding to the $\alpha\beta$ bond configuration. Then the contribution to the density matrix provided by the transition from configuration 1 to configuration 2 assumes the form

$$\frac{\prod_\alpha g_\alpha}{\prod_\beta g_\beta}\,\frac{W'(1)}{W}\,, \quad (52)$$

where the first cofactor is the ratio of the amplitude of configuration 1 to the amplitude of configuration 2, i.e., g_α corresponds to the bonds in configuration 2 that were absent in configuration 1, and g_β corresponds to the opposite situation. If configurations 1 and 2 differ only in several identical bonds, the parameters g_α and g_β enter into Eqn (51) raised to the corresponding powers. On the whole, the procedure is similar to Gutzwiller's method [15, 66], where Eqn (52) contained only one parameter g_0.

Using the expressions (51) and (52), we can directly sum all the configurations and calculate the density matrix (50):

$$\rho_1 = 4\left[2y_4(a_1a_2)^{z-1} + \frac{y_3g_7}{g_0g_3}\,a_1^{2(z-1)} + \frac{y_7g_0g_3}{g_7}\,a_2^{2(z-1)}\right], \quad (53)$$

where

$$a_1 = \frac{y_2g_4 + y_3g_4/g_3 + y_4(g_7+1)/g_4}{x}$$

and

$$a_2 = \frac{y_6g_4 + y_7g_4/g_7 + y_4(g_3+1)/g_4}{(1/2-x)}\,.$$

Here and below we use y_2 and y_6 instead of expressions (47) to make the notation more compact. As in Gutzwiller's method, there are three terms in the density matrix, with the first describing fermion motion in the Hubbard subband, and the second and third describing the transitions between subbands. Let us use Eqn (49) to exclude the parameters g_i from Eqn (53). Direct transformations then yield [22]

$$\rho_1 = 8\left(y_4 + \sqrt{y_3y_7}\right) \times\left[\frac{y_4}{x(1/2-x)}\left(\sqrt{y_2}+\sqrt{y_3}+\sqrt{y_6}+\sqrt{y_7}\right)^2\right]^{z-1}. \quad (54)$$

It is convenient to write the final expression for the total energy of a system of fermions in Gutzwiller's form [15]

$$E = \frac{1}{L}\,\frac{\langle\psi|H|\psi\rangle}{\langle\psi|\psi\rangle} = q\varepsilon_0 + xU\,, \quad (55)$$

where $q = \rho_1/\rho_1^0$, ρ_1^0 is the value of the density matrix of uncorrelated electrons, i.e., calculated at $U = 0$, and ε_0 is the average energy of the uncorrelated electrons. Such normalization corresponds to procedure (42). Thus, we have an analytical expression for the energy of a strongly correlated system in analytical form as a function of the variational variables.

The ground-state energy can be found by minimizing the energy (55) in the four variables x, y_3, y_4, and y_7. The search for the global minimum was carried out numerically (an improved Nelder–Mead simplex method) and presented no difficulties because expression (55) is a smooth differentiable function without singularities inside its domain.

Figure 8 shows the results of calculations of the ground-state energy of the PM phase for a linear homogeneous chain

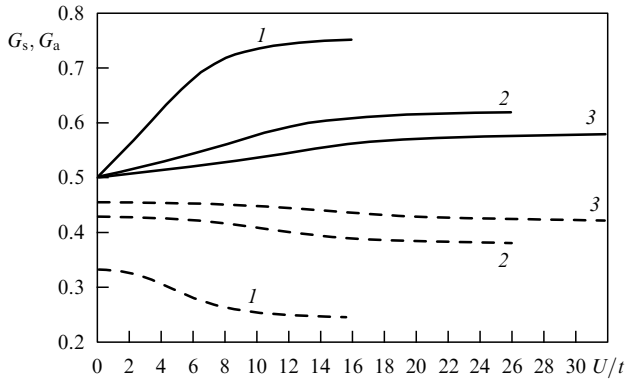

Figure 12. Symmetric G_s (dashed curves) and antisymmetric G_a (solid curves) correlation functions (56) for a 1D chain (*1*), a two-dimensional square lattice (*2*), and a simple cubic lattice (*3*) [21, 22].

with $z = 2$ and a dispersion law $\varepsilon_{\mathbf{k}} = -2\cos k_x$ (Fig. 8a), for a two-dimensional square lattice with $z = 4$ and $\varepsilon_{\mathbf{k}} = -2(\cos k_x + \cos k_y)$ (Fig. 8b), and for a simple cubic lattice with $z = 6$ and $\varepsilon_{\mathbf{k}} = -2(\cos k_x + \cos k_y + \cos k_z)$ (Fig. 8c). Figure 12 depicts the symmetric and antisymmetric correlation functions of a pair of nearest-neighbor sites for different lattices:

$$\begin{aligned} G_s &= \langle n_\uparrow n_\uparrow \rangle' + \langle n_\downarrow n_\downarrow \rangle' = 2(y_2 + 2y_4 + y_6)\,, \\ G_a &= \langle n_\uparrow n_\downarrow \rangle' + \langle n_\downarrow n_\uparrow \rangle' = 2(y_2 + 2y_4 + y_7)\,. \end{aligned} \tag{56}$$

The prime in Eqn (56) stands for an average over the nearest neighbors. Note that at $U = 0$ there are no correlations between fermions of opposite spins ($G_a = 0.5$), while in the case of fermions of the same spin an exchange hole emerges ($G_a < 0.5$). This effect emerged quite naturally as a result of the variational procedure.

In order to study the limit $D = \infty$ in the PM phase, the ground-state energies for hypercubic lattices with $z = 50, 100, 200, 400$, and 1000 were calculated [22]. As the dimensionality of the lattice increased, the ground-state energy tended to Gutzwiller's solution, which is the exact solution at $D = \infty$. At $z = 1000$ both solutions coincided to within 0.1% with U in the interval $[0,\ U_C/2]$ and to within 1% with U in the interval $[U_C/2,\ 0.8U_C]$, where $U_C = 8\varepsilon_0$.

It is a good idea to compare the results of calculations of the ground-state energy done by the variational cluster method with those obtained by the variational Monte Carlo method [20] (see Figs 8 and 9). As we remarked in Section 3.3, calculations done by the variational Monte Carlo method are based on the Gutzwiller trial function, i.e., nonlocal correlations are practically ignored. In Reference [22] the ground-state energy was found for a trial function that explicitly incorporated nearest-neighbor correlations on the lattice. In our model, larger-radius correlations obey the superposition hypothesis [1]. Thus, the difference in the ground-state energies in these two methods emerges because of short-range correlations between fermions in the ground state. For a one-dimensional chain (Fig. 8a) this difference is insignificant, and the results obtained by the variational Monte Carlo method are not shown in the diagram. But in the cases of a two-dimensional square lattice and a simple cubic lattice in the PM phase (Figs 8b and c), it becomes obvious that near U_C the ground-state energy of the trial wave function with SRO (35) is much lower (by a factor of two to three) than the energy calculated by the variational Monte Carlo method. Thus, in the PM phase, SRO significantly lowers the ground-state energy of 2D and 3D lattices and becomes the leading factor in a strongly correlated state. Actually, the variational Monte Carlo method [20] and the analytical $1/D + 1/D^2$ expansion [70] in this case yield incorrect results.

In contrast to the well-known Hubbard-III approximation [14, 93], in the variational theory of SRO short-range AFM correlations do not disappear in the limit $U \gg \Delta$. This agrees with the fact that in this limit the Hubbard model with half band-filling coincides with the Heisenberg model of spin 1/2. The values of the correlation functions in Fig. 12 for large values of U agree with the results of studies of the ground state of the Heisenberg model [94].

While comparing the theoretical results with the experimental data (see Section 2), it is a good idea to formulate our results [21, 23] in terms of the correlation length. To this end, in addition to the correlation functions (56) we introduce the correlation function $G_b = G_s - G_a$. Here and below we use such a normalization of the correlation functions so that $G_b = 1$ for ferromagnetic orientation of the spins in a pair and $G_b = -1$ for the antiferromagnetic orientation. According to the superposition hypothesis [1], the correlation function of a pair of next-nearest neighbors amounts to G_b^2, while for the nth neighbors it amounts to G_b^n. In this case the correlations decay according to an exponential law, $\propto \exp(-r/\xi)$, where the correlation length $\xi = a/|\ln G_b|$, with a the nearest-neighbor distance. Then Figure 12 suggests that for large values of U we have $\xi = 1.4a$ for a one-dimensional chain, $\xi = 0.7a$ for a two-dimensional square lattice, and $\xi = 0.55a$ for a simple cubic lattice. According to optical measurements [95], we can assume that the band width for V_2O_3 in the metallic PM phase is roughly 0.5 eV, while $U \approx 1$ eV. Then the estimate $\xi = 0.55a$ is in satisfactory agreement with the results of neutron scattering measurements [5].

In Reference [22] the ground-state energy of the AFM phase in the Hubbard model with half filling was calculated in roughly the same way as described above. The main difference was in the way the trial wave function and set of operators Y_λ were selected. For the trial wave function for the AFM phase to have the necessary translational properties, we take the Hartree–Fock wave function of the AFM metal, $|\varphi_0^{\mathrm{AFM}}\rangle$ [20, 96] as the initial wave function. Then the energy spectrum of the initial wave function and the magnetic moment of the sublattices assume the form [96]

$$\varepsilon_{\mathbf{k}}^{\mathrm{AFM}} = \frac{\varepsilon_{\mathbf{k}}}{\sqrt{1 + (\delta/\varepsilon_{\mathbf{k}})^2}}\,, \qquad m = \int \frac{\delta\, \mathrm{d}\mathbf{k}}{\sqrt{\varepsilon_{\mathbf{k}}^2 + \delta^2}}\,, \tag{57}$$

where $\varepsilon_{\mathbf{k}}$ is the energy spectrum of uncorrelated fermions of the PM phase, δ is the AFM order parameter, integration is over the irreducible Brillouin zone [96], and $m = (\langle n_\uparrow \rangle_A + \langle n_\downarrow \rangle_B - \langle n_\downarrow \rangle_A - \langle n_\uparrow \rangle_B)/2$. In the last expression, the averaging is done over the sites of the sublattices A and B. In the AFM phase, the degeneracy of the operators Y_λ is partially lifted and their number increases.

The results of calculations of the ground-state energy of the AFM phase are shown in Fig. 9. What is interesting is that in the AFM phase they practically coincide with those of calculations by the variational Monte Carlo method [20]. Deviations are no greater than 1%. Thus, no SRO develops in the AFM phase, and the Gutzwiller wave function yields a good solution.

The PM phase with half band-filling in a magnetic field has been studied in Ref. [99]. In this case the average kinetic energy of noninteracting fermions depends on the magnetic moment, $\varepsilon_0(m)$, and the set of operators expands in comparison to the set listed in Table 2. The main goal of Ref. [99] was to study a metamagnetic transition in magnetic field. For an infinite-dimensional lattice placed in magnetic field there emerges a first-order phase transition [67]. On the other hand, the phase transition that emerges in the absence of a magnetic field at critical U_C is a special feature of an infinite-dimensional lattice. Hence it is not obvious that the metamagnetic transition in magnetic field in Gutzwiller's theory correctly reflects the situation for finite-dimensional lattices. As a result of calculations of the ground-state energy with allowance for SRO it was found that in the Hubbard model with half band-filling the metamagnetic transition emerged in a one-dimensional chain and a two-dimensional lattice but did not emerge in a simple cubic lattice [99]. This points to the essential role of the dimensionality and structure of the lattice.

The above examples illustrate the main ways in which the initial wave function and the set of operators $\widehat{Y}_\lambda$ should be chosen: (1) the trial wave function must satisfy the symmetry requirements of the phase for which the calculation is being done, and (2) the set of the operators $\widehat{Y}_\lambda$ must, on the one hand, be as extended as possible but, on the other hand, must not break the symmetry of the phase.

In concluding this section, we note that two simplifications were employed in the proposed theory. First, we ignored boundary effects and, second, in calculating W we did not take into account closed paths on the lattice. However, within the VCM theory we can examine not only pair correlations but also more complex models, e.g., correlations of three or more sites [83]. The augmentation of the cluster gradually leads to inclusion of closed paths on the lattice. Moreover, we can examine a sequence of approximate solutions: Gutzwiller's theory (the cluster consists of a single site) as the zeroth approximation, the trial wave function (28) (the cluster consists of a pair of sites) as the first approximation, and so on. What is important is that for a sequence of such approximations there is rigorous proof of convergence to the exact solution in the two- and three-dimensional cases [84].

4.4 Elementary excitation spectrum of a strongly correlated system

The energy spectrum of the quasiparticles is one of the central problems of the theory of strongly correlated states. Many research papers and reviews have been devoted to it (e.g., see Refs [4, 8–12, 67, 68, 74, 50, 97, 98]). In this section we will concentrate on the problem of one-particle excitations in the variational theory of SRO. There are two ways in which excited states of a strongly correlated system can be obtained in the variational theory. We begin with the spectrum of coherent excitations. Suppose that the initial state $|\varphi_0\rangle$ is the Fermi sea of noninteracting fermions (20). We create an excited uncorrelated state $a^+_{\mathbf{k}\sigma}|\varphi_0\rangle$ that has a wave vector $\mathbf{k}$ and energy $\varepsilon_\mathbf{k}$. If we now use the new state as the initial one and apply the variational procedure similar to the one used to determine the ground state, we arrive at a new correlated state with the same the wave vector $\mathbf{k}$ (since the operator $\widehat{F}$ is translation-invariant) and a minimum energy in the class of trial functions with the wave vector $\mathbf{k}$. Since the wave vector and energy of the new state are well-defined, it is only natural to take the new state as a quasiparticle excited state.

This procedure can be formulated in terms of the Fermi-liquid theory in the same way as it has been done in the theory of an almost localized Fermi liquid [67]. The variation of the system's energy caused by a small deviation of the distribution function from the equilibrium distribution can be written as follows:

$$\delta E = \varepsilon_0 \sum_\lambda \sum_{\mathbf{k}\sigma} \frac{\partial q}{\partial y_\lambda} \frac{\partial y_\lambda}{\partial n_\sigma} \delta n_{\mathbf{k}\sigma} + \sum_{\mathbf{k}\sigma} \left(\varepsilon_0 \frac{\partial q}{\partial x} + U \right) \frac{\partial x}{\partial n_\sigma} \delta n_{\mathbf{k}\sigma} + q \sum_{\mathbf{k}\sigma} \varepsilon^0_{\mathbf{k}\sigma} \delta n_{\mathbf{k}\sigma} + \varepsilon_0 \sum_{\mathbf{k}\sigma} \frac{\partial q}{\partial n_\sigma} \delta n_{\mathbf{k}\sigma} , \quad (58)$$

where $\delta n_{\mathbf{k}\sigma}$ is the variation of the distribution function, and $\varepsilon^0_{\mathbf{k}\sigma} = \partial\varepsilon_0/\partial n_{\mathbf{k}\sigma}$ is the spectrum of excitations of the uncorrelated system of particles, i.e., at $U = 0$. The index λ runs through values corresponding to the independent variables. Clearly, the first and second terms on the right-hand side of Eqn (58) vanish in view of the requirement that the ground-state energy must be at its minimum in the variational parameters. The remaining expression coincides exactly with the expression obtained in the theory of an almost localized Fermi liquid [67]:

$$\delta E = q \sum_{\mathbf{k}\sigma} \varepsilon^0_{\mathbf{k}\sigma} \delta n_{\mathbf{k}\sigma} + \varepsilon_0 \sum_{\mathbf{k}\sigma} \frac{\partial q}{\partial n_\sigma} \delta n_{\mathbf{k}\sigma} . \quad (59)$$

The first term on the right-hand side of Eqn (59) is the spectrum of the system of noninteracting particles 'compressed' by the factor q. The second term was interpreted in the theory of an almost localized Fermi liquid for ^{3}He as the term responsible for interaction in Landau's theory [67]. Indeed, the partial derivative in this term describes the variation of the distribution function. For ^{3}He this 'interaction' varies under changes of external pressure, density, etc. For crystalline solids $\varepsilon_0 \partial q/\partial n_\sigma$ is constant. Moreover, we see that it is independent of the wave vector. Thus, in our case the second term on the right-hand side of Eqn (59) simply describes the displacement of the spectrum by a constant quantity and is insignificant. The final expression for the quasiparticle spectrum is

$$\varepsilon_{\mathbf{k}\sigma} = q\varepsilon^0_{\mathbf{k}\sigma} . \quad (60)$$

The spectrum is narrowed by the factor q. The density of states and the effective mass increase in proportion to g^{-1}. Figure 13 shows the dependence on U of the effective electron mass in the PM phase in the Hubbard model with half band-filling. The quasiparticle spectrum (60) coincides in form with the spectrum obtained by the auxiliary boson method [64] and in the theory of an almost localized Fermi liquid [102, 103].

Incoherent excitations can also be studied by the variational model. To this end we create the excited state $a^+_{i\sigma}|\psi\rangle$, where $|\psi\rangle$ is the ground state of the correlated system [Eqn (28)]. Such an excited state corresponds to a sudden switch-on of the perturbation, in contrast to the adiabatic switch-on discussed in equations (58)–(60). The evolution of the excited state $a^+_{i\sigma}|\psi\rangle$ can be studied, say, by the method of equations of motion for Green's function. The simplest example here is the Hubbard-I approximation [104]. Actually, the difference between the Hubbard-I approximation and the standard approximation is the ground state. Instead of the PM state of noninteracting fermions we use $|\psi\rangle$ which is determined by the variational procedure and contains dynamical correlations. Note that in deriving the equations

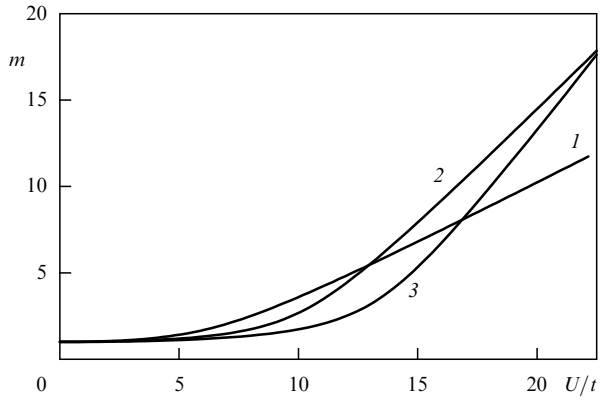

Figure 13. Effective quasiparticle mass in the Hubbard model in the PM phase: *1* — one-dimensional chain, *2* — square lattice, and *3* — simple cubic lattice.

of motion one has to use only the properties of the creation and annihilation operators in Green's function, with the result that the equations of motion are the same as in Ref. [104]:

$$E\Gamma^{\sigma}_{ij} = \frac{1}{2\pi}\,\delta_{ij}\langle n_{i,-\sigma}\rangle + U\Gamma^{\sigma}_{ij} + \sum_{l\neq i} t_{il}\big\langle\langle n_{i,-\sigma}\,a_{l\sigma};a^{+}_{j\sigma}\rangle\big\rangle_E + \sum_{l\neq i} t_{il}\Big(\big\langle\langle a^{+}_{i,-\sigma}\,a_{l,-\sigma}\,a_{i\sigma};a^{+}_{j\sigma}\rangle\big\rangle_E - \big\langle\langle a^{+}_{l,-\sigma}\,a_{i,-\sigma}\,a_{i\sigma};a^{+}_{j\sigma}\rangle\big\rangle_E\Big), \tag{61}$$

where $\Gamma^{\sigma}_{ij} = \langle\langle n_{i,-\sigma}\,a_{i\sigma};a^{+}_{j\sigma}\rangle\rangle_E$, $\langle\langle\ldots;\ldots\rangle\rangle_E$ is Green's function in the notation of Refs [104, 105]. The difference lies in the decoupling of the two-particle Green's functions. In the Hubbard-I approximation, the last term on the right-hand side of Eqn (61) is ignored and the third term is approximately written as follows:

$$\big\langle\langle n_{i,-\sigma}\,a_{l\sigma};a^{+}_{j\sigma}\rangle\big\rangle_E \approx \langle n_{i,-\sigma}\rangle\big\langle\langle a_{l\sigma};a^{+}_{j\sigma}\rangle\big\rangle_E . \tag{62}$$

This means that there are no correlations in the ground state between fermions with oppositely directed spins on neighboring lattice sites, which is true for the PM state of noninteracting electrons to within higher-order corrections. On the other hand, such correlations exist in the ground state $|\psi\rangle$. Hence we must replace Eqn (62) with

$$\big\langle\langle n_{i,-\sigma}\,a_{l\sigma};a^{+}_{j\sigma}\rangle\big\rangle_E \approx C\langle n_{i,-\sigma}\rangle\big\langle\langle a_{l\sigma};a^{+}_{j\sigma}\rangle\big\rangle_E , \tag{63}$$

where $C = \langle n_{i,-\sigma}(1-n_{l\sigma})\rangle/\langle n_{i,-\sigma}\rangle\langle 1-n_{l\sigma}\rangle$ is a correction factor that allows for SRO in the ground state. In the Hubbard-I approximation, the effect of SRO on the excitation spectrum is purely quantitative. This example shows that the methods of equations of motion may be carried over to the variational model with corrections that emerge because of SRO.

It would be interesting to analyze the properties of the system at low (but finite) temperatures. The behavior of the trial variational function (28) at finite temperatures can be studied by the variational cluster method [85]. This requires time-consuming calculations. On the other hand, a less rigorous but much simpler approach can be used here, an approach that was used earlier for studying the thermodynamics of an almost localized Fermi liquid [102, 103]. To calculate the free energy at low temperatures, we introduce the dimensionless variables [103]

$$\xi = \frac{2\varepsilon}{\Delta},\quad t = \frac{2k_{\mathrm{B}}T}{\Delta},\quad h' = \frac{2h}{\Delta},\quad f = \frac{2F}{\Delta},\quad v = \frac{2\varepsilon_{\mathrm{F}}}{\Delta}, \tag{64}$$

where Δ is the width of the initial band. It can be demonstrated that if the ground-state energy has the form (55), the free energy of a correlated system can be expressed as follows [102, 103]:

$$f_{\mathrm{c}} = qf_0 + ux\,, \tag{65}$$

where the free energy of the uncorrelated system

$$f_0\left(\frac{t}{q},v\right) = \sum_{\sigma}\int_{-1}^{1}\rho(\xi)\times\left\{n_\sigma\,\xi + \frac{t}{q}\left[n_\sigma\ln n_\sigma + (1-n_\sigma)\ln(1-n_\sigma)\right]\right\}\mathrm{d}\xi\,. \tag{66}$$

Here the concentration of particles with spin σ is

$$n_\sigma = \left[1+\exp\frac{q(\xi-v_\sigma)}{t}\right]^{-1}.$$

Assuming that the density of states is known (for a one-dimensional chain and a two-dimensional lattice it is known in analytic form), we can calculate f_0. The calculation of f_{c} is very similar to the calculation of the ground-state energy.

4.5 Ground state of the Kondo – Hubbard lattice

The interaction of itinerant electrons and the lattice of localized states may lead to a special correlated state, heavy fermions [3, 59, 68, 106, 107]. This phenomenon is usually observed in f-metal compounds. Sometimes heavy fermions may emerge in d-metal compounds, e.g., in Li_2O_4 [32]. In many cases the initial conduction band in these substances is formed by d-electrons, with the result that, in addition to taking into account the exchange interaction of itinerant electrons and localized electrons, we must allow for the Hubbard interaction. Both types of interaction are incorporated into the Kondo – Hubbard model [100]. Let us consider two species of fermions on the lattice: mobile fermions with strong short-range interaction, i.e., described by the Hubbard Hamiltonian, and localized fermions. If a localized state has a frozen-in orbital angular momentum and spin 1/2, which is typical of localized d-states, the Kondo – Hubbard Hamiltonian can be written as follows [100]:

$$H_{\mathrm{KH}} = H_{\mathrm{H}} + J\sum_i \mathbf{S}^{\mathrm{l}}_i\cdot\mathbf{S}^{\mathrm{c}}_i\,, \tag{67}$$

where H_{H} is the Hubbard Hamiltonian (8) of the itinerant electrons, and $\mathbf{S}^{\mathrm{l(c)}}_i$ is the spin operator for a localized electron (itinerant electron) with spin 1/2. Below we assume the exchange in Eqn (67) is antiferromagnetic, i.e., $J>0$. It is convenient to represent such a system by the equivalent lattice shown in Fig. 11b. Note that there are no additional closed paths on such a lattice (compared to the lattice depicted in Fig. 11a), with the result that no new simplifying assumptions have been introduced into the variational theory of SRO.

The trial wave function of the Kondo – Hubbard lattice has the general form [101]

$$|\psi\rangle = \prod_\lambda g_\lambda^{\hat{P}_\lambda}\prod_\zeta g_\zeta^{\hat{P}_\zeta}|\varphi_{\mathrm{c}}\rangle|\varphi_{\mathrm{f}}\rangle = \prod_\zeta g_\zeta^{\hat{P}_\zeta}|\psi_{\mathrm{c}}\rangle|\varphi_{\mathrm{f}}\rangle\,. \tag{68}$$

Here $|\varphi_c\rangle$ is the wave function of noninteracting itinerant electrons (see Section 4.1), $|\psi_c\rangle$ is the trial wave function of the Hubbard model [Eqn (28)], $|\varphi_f\rangle$ is the wave function of noninteracting localized fermions, and $\widehat{P}_\zeta$ and g_ζ are the set of projection operators and the corresponding variational parameters of the Kondo part of the trial function.

Below we do the calculations for the PM phase of the Kondo – Hubbard model with half conduction-band-filling. We examine the states of a pair consisting of a localized electron and an itinerant electron on a single lattice site. There are three possible configurations of such a pair in the PM phase: singlet, triplet, and with a zero total spin of itinerant electrons on the site (Table 3). We denote the eigenvalues of the operators by r_1, r_2, and r_0. For these eigenvalues we can write two self-consistency conditions:

$$r_0 = \frac{1}{2}\,x\,, \qquad r_1 + r_2 = \frac{1}{2} - x\,. \tag{69}$$

Table 3. Configurations of a localized-state – delocalized-state pair at a single site on the Kondo – Hubbard lattice (spin 1/2, PM phase, half band-filling).

Eigenvalue	Configuration		Degeneracy multiplicity
	Delocalized state	Localized state	
$x/2$	$S = 0$	$\uparrow$	2
r	$\uparrow$	$\downarrow$	2
$1/2 - x - r$	$\uparrow$	$\uparrow$	2

This implies that we must augment the independent parameters describing the itinerant electrons ($x = x_1 = x_4$, y_3, y_4, and y_7) with a new independent parameter $r = r_1$. In this case we can write the trial wave function of the Kondo – Hubbard lattice as follows:

$$|\psi_{KH}\rangle = g_r^{\beta_r\hat{\mathfrak{R}}}|\psi_H\rangle|\varphi_f\rangle = g_r^{\beta_r\hat{\mathfrak{R}}} g_0^{\hat{X}}\, g_3^{\beta_3\hat{Y}_3}\, g_4^{4\beta_4\hat{Y}_4}\, g_7^{\beta_7\hat{Y}_7}|\varphi_c\rangle|\varphi_f\rangle\,. \tag{70}$$

Here $|\psi_H\rangle$ is the trial wave function of the Hubbard model in the PM phase [Eqn (35)], and $\hat{\mathfrak{R}} = -4\sum_i S_{zi}^{l}\, S_{zi}^{c}$, $S_{zi}^{c(l)}$ is the z-projection of the spin. The norm of the trial wave function can be separated into two parts,

$$\langle\psi|\psi\rangle = \sum_{\{r,x,y_3,y_4,y_7\}} W^{K}_{\{x,r\}}\, W^{H}_{\{x,y_3,y_4,y_7\}}\, g_r^{4Lr} g_0^{2Lx} g_3^{2zLy_3} \times g_4^{8zLy_4} g_7^{2zLy_7} = \sum_{\{r,x,y_3,y_4,y_7\}} R_{\{r,x,y_3,y_4,y_7\}}, \tag{71}$$

where $W^{K(H)}$ is the Kondo (Hubbard) part of W. The Hubbard part W^{H} is known [see equation (43)], while the Kondo part can easily be calculated:

$$W^{K} = \frac{(2xL)!}{\big[(xL)!\big]^2}\,\left\{\frac{\big[L(1/2-x)\big]!}{(rL)!\big[(1/2-x-r)L\big]!}\right\}^2. \tag{72}$$

Next we look for the global maximum in the same way as we did in Section 4.3 and arrive at the equation $\partial(\ln R)/\partial\eta_\lambda = 0$, where $\eta_\lambda = r, x, y_3, y_4, y_7$. The equations for y_3, y_4, and y_7 are the same as in the Hubbard model [Eqns (49)], while for the other parameters we have

$$g_0 = \frac{1/2-x}{2\sqrt{r(1/2-x-r)}}\left(\frac{1/2-x}{x}\right)^{z-1} \times \left(\frac{x-y_3-2y_4}{1/2-x-y_7-2y_4}\right)^{z/2}, \qquad g_r = \left(\frac{r}{1/2-x-r}\right)^{1/4}. \tag{73}$$

Since the hopping of the itinerant electron changes the configuration of the pair consisting of an itinerant electron and a localized electron at a single site, the density matrix of the Hubbard terms [Eqn (54)] changes. Now instead of Eqn (54) we have [101]

$$\rho_H = 4\left[2y_4(a_1a_2)^{z-1}b_1b_2 + \frac{y_3g_7}{g_0g_3}\,a_1^{2(z-1)}b_2^2 + \frac{y_7g_0g_3}{g_7}\,a_2^{2(z-1)}b_1^2\right], \tag{74}$$

where

$$b_1 = \frac{r}{g_r} + g_r\left(\frac{1}{2}-x-r\right), \qquad b_2 = \frac{1}{2}\left(g_r + g_r^{-1}\right).$$

After direct calculations the zz and spin-flip terms in the density matrix assume the form

$$\rho_{zz} = -\frac{1}{2}\left(2r + x - \frac{1}{2}\right), \qquad \rho_{\pm} = -r\,\frac{2y_4 + y_6g_7 + y_7g_7^{-1}}{(1/2-x)^z}\,. \tag{75}$$

The total energy of the fermion system can be written in the form (55)

$$E = \frac{1}{L}\,\frac{\langle\psi|H|\psi\rangle}{\langle\psi|\psi\rangle} = q\varepsilon_0 + xU + J(\rho_{zz} + \rho_{\pm})\,, \tag{76}$$

where $q = \rho_H/\rho_H^0$, with ρ_H^0 the value of the Hubbard part of the density matrix at $U = 0$. Next we determine the ground-state energy by minimizing the function (76) in the variables r, x, y_3, y_4, and y_7. Figures 14 and 15 show the Kondo-singlet fraction $2r$ and the correlation functions of the itinerant electrons,

$$G_b = 2\langle S_{zi}^{c}\, S_{zj}^{c}\rangle' = 2(y_6 - y_7)\,, \tag{77}$$

and a pair of nearest-neighbor localized states,

$$G_l = 8\langle S_{zi}^{c}\, S_{zj}^{c}\rangle'\langle S_{zi}^{c}\, S_{zi}^{l}\rangle^2 = 2(y_6-y_7)(1-2x-4r)^2\,. \tag{78}$$

Formula (78) follows from the superposition hypothesis [1]. Figure 16 depicts the dependence of the effective quasiparticle mass $m = q^{-1}$ on J.

Keeping in mind the Kondo – Hubbard lattices with cerium ions (Ce^{3+}), we generalize the above results to a lattice of localized states with a total angular momentum equal to 5/2. The Hamiltonian (67) formally retains the

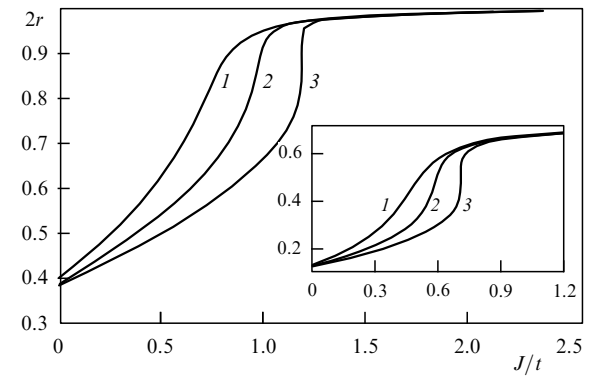

Figure 14. Fraction $2r$ of Kondo singlets in the Kondo–Hubbard model with spin 1/2 ($U = 0.5U_C$): *1* — one-dimensional chain, *2* — square lattice, and *3* — simple cubic lattice. The inset shows the same for the f-spin 5/2 [101].

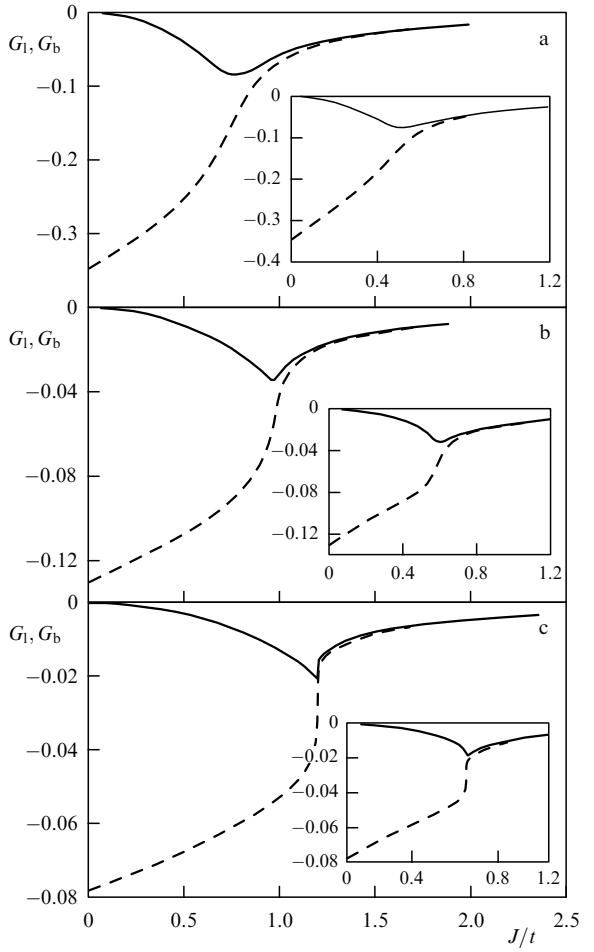

Figure 15. Correlation functions G_l (solid curves) and G_b (dashed curves) in the Kondo–Hubbard model with spin 1/2 ($U = 0.5U_C$): (a) one-dimensional chain, (b) square lattice, and (c) simple cubic lattice. The insets show the same for the f-spin 5/2 [101].

previous form, only here $\mathbf{S}_i^l$ is interpreted as the total magnetic moment (the f-spin operator [100]). We also note that we have ignored the splitting of the multiplet by the crystalline field, i.e., we assume that the field is weak compared to the exchange interaction J.

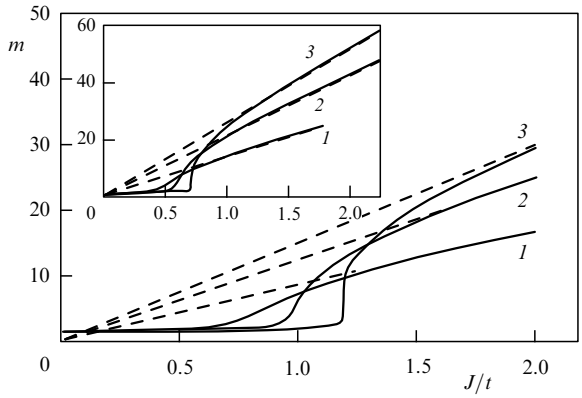

Figure 16. Effective quasiparticle mass in the Kondo–Hubbard model with spin 1/2 at $U = 0.5U_C$ (solid curves): *1* — one-dimensional chain, *2* — square lattice, and *3* — simple cubic lattice. The inset shows the same for the f-spin 5/2 [101].

Let us set up a table of the possible configurations of the total angular momenta of a localized electron and an itinerant electron at a single lattice site (Table 4). The probabilities that different configurations with a zero spin of the itinerant electrons will appear at the site are all the same, in view of invariance under rotations, i.e., $r_0 = x/6$. In contrast to the case of a localized impurity with spin 1/2, we have six configurations r_i with a nonzero spin of the itinerant electron. The configurations are related through the normalization condition

$$\sum_{i=1}^{6} r_i = \frac{1}{2} - x\,. \tag{79}$$

Then only five parameters are independent; for instance, we can assume that r_6 is not independent. For the trial variational function we take the natural generalization of formula (70) for spin 5/2. The meaning of this ansatz can be understood by analogy with the Gutzwiller trial function. If the exchange interaction is of an AFM nature, the configuration with antiparallel moments of the localized state and the itinerant electron, $S_{zi}^l S_{zi}^c = -6$, has a maximum amplitude. As the product $S_{zi}^l S_{zi}^c$ increases, the state amplitude decreases. The norm of the trial wave function has the form

$$\langle\psi|\psi\rangle = \sum_{\{r_i, x, y_3, y_4, y_7\}} W^{\mathrm{K}}_{\{x, r_i\}} W^{\mathrm{H}}_{\{x, y_3, y_4, y_7\}} g_r^{4L\sum_{i=1}^{6} r_i(7-2i)} \times g_0^{2Lx} g_3^{2zLy_3} g_4^{8zLy_4} g_7^{2zLy_7}\,. \tag{80}$$

Table 4. Configurations of a localized-state–delocalized-state pair at a single site on the Kondo–Hubbard lattice (spin 5/2, PM phase, half band-filling).

Eigenvalue	Configuration		Degeneracy multiplicity
	Delocalized state	Localized state	
$x/6$	$S = 0$	any	2
r_1	1/2	−5/2	2
r_2	1/2	−3/2	2
r_3	1/2	−1/2	2
r_4	1/2	1/2	2
r_5	1/2	3/2	2
$r_6 = 1/2 - x - \sum_{i=1}^{5} r_i$	1/2	5/2	2

The Kondo part of the configuration's weight in the case $J = 5/2$ is reduced to

$$W^{\mathrm{K}} = \frac{(2xL)!}{[(xL)!]^6} \left\{ \frac{[L(1/2-x)]!}{\prod_i (r_i L)!} \right\}^2 . \tag{81}$$

Minimization in the independent parameters, $\partial(\ln R)/\partial\eta_\lambda = 0$, where $\eta_\lambda = r_i, x, y_3, y_4, y_7$, leads to nine equations. In particular, for the five independent variables r_i we have five equations

$$g_r^{4(6-i)} = \frac{r_i}{r_6} , \tag{82}$$

where $r_6 = 1/2 - x - \sum_{i=1}^{5} r_i$. This implies that actually among the r_i there is only one independent parameter,[2] r_i, e.g., $r = r_1$. As a result of simple manipulations we arrive at a nonlinear equation that relates g_r and r:

$$r(1 + g_r^{-4} + g_r^{-8} + g_r^{-12} + g_r^{-16} + g_r^{-20}) = \frac{1}{2} - x . \tag{83}$$

The equation for g_0 becomes

$$g_0 = \frac{1/2 - x}{6\sqrt{r r_6}} \left(\frac{1/2 - x}{x} \right)^{z-1} \left(\frac{x - y_3 - 2y_4}{1/2 - x - y_7 - 2y_4} \right)^{z/2} . \tag{84}$$

And again, the equations for y_3, y_4, and y_7 are the same as in the Hubbard model [Eqns (49)].

As in the case of a localized impurity of spin 1/2, the density matrix can be divided into the Hubbard, zz, and spin-flip parts. The general form of the Hubbard term remains the same [see Eqn (74)], where

$$\begin{aligned} b_1 &= \frac{\sum_{i=1}^{3} (g_r^{2i-1} + g_r^{1-2i})}{6} , \\ b_2 &= \frac{r \sum_{i=1}^{6} g_r^{-3-2i}}{1/2 - x} . \end{aligned} \tag{85}$$

Direct calculations lead to expressions for the zz and spin-flip terms:

$$\begin{aligned} \rho_{zz} &= -\frac{1}{2} \sum_{i=1}^{6} r g_r^{4(1-i)} (7 - 2i) , \\ \rho_{\pm} &= -(1 - 2x - r g_r^{-20})\, g_r^{-2} . \end{aligned} \tag{86}$$

The energy of the electron system can now be written in the form (76). The ground-state energy is determined via minimization in five variational parameters. Certain complications arise in the numerical calculations, since the parameter g_r cannot be analytically expressed in terms of r. But, on the whole, the procedure is similar to the case of spin 1/2. The insets in Figs 14 and 15 show the diagrams for the function $2r$ and the correlation functions of itinerant electrons (77) and the nearest localized neighbors:

$$\begin{aligned} G_1 = \langle S_{zi}^{\mathrm{c}} S_{zj}^{\mathrm{c}} \rangle' \big(\langle S_{zi}^{\mathrm{c}} S_{zi}^{1} \rangle \big)^2 = \frac{8}{25} (y_6 - y_7)\, r^2 \times \\ \times \left[5(1 - g_r^{-20}) + 3(g_r^{-4} - g_r^{-16}) + g_r^{-8} - g_r^{-12} \right]^2 . \end{aligned} \tag{87}$$

The dependence of the effective mass $m = q^{-1}$ on J is shown in the inset in Fig. 16.

[2] The reason is that in the trial function we used only one parameter g_r.

Two types of fermion behavior as a function of J are quite obvious from Figs 14 – 16. For small values of J (the Hubbard regime), the exchange interaction has only a small effect on the ground state energy and the effective quasiparticle mass. A characteristic feature of this regime is a buildup of the AFM correlations between the nearest neighbors (G_1). This effect emerges because AFM correlations of itinerant electrons exist even at $J = 0$ (Hubbard correlations). Then for small values of J the states of localized electrons would seem to follow the band correlations. As J increases, the band AFM correlations become suppressed, and a transition to a new regime (a Kondo lattice) takes place. For large values of J, the effective quasiparticle mass rapidly grows, and the AFM correlations of both band and localized states are suppressed. The ground-state energy tends to the limit of coupled Kondo singlets (for spin 1/2 this limit is $-(3/4)J$). Figure 14 shows that the fraction of singlets ($2r$) for spin 1/2 tends to 1, while for spin 5/2 the function $2r$ tends to a limit smaller than 1. The reason is that the ground state of a pair of localized spins $S = 5/2$ and $S = 1/2$ coupled by Heisenberg exchange incorporates, in addition to the states $|S_z^{\mathrm{l}} = 5/2\rangle |S_z^{\mathrm{b}} = -1/2\rangle$ and $|S_z^{\mathrm{l}} = -5/2\rangle |S_z^{\mathrm{b}} = 1/2\rangle$, states of the type $|S_z^{\mathrm{l}} = 3/2\rangle |S_z^{\mathrm{b}} = -1/2\rangle$, $|S_z^{\mathrm{l}} = -3/2\rangle |S_z^{\mathrm{b}} = 1/2\rangle$, etc. (with smaller weights, however). The tendency towards development of AFM correlations between localized states at small values of J and suppression of such correlations at large values of J is characteristic of Doniach's diagram [47]. What is interesting here, however, is that we did not introduce the RKKY interaction into our scheme, i.e., the nature of the nonmonotonic dependence of the AFM correlations of the nearest localized neighbors differs from the one proposed by Doniach [47]. Building a complete physical picture also requires examining the AFM phase of the Kondo lattice (this has yet to be done).

The Hamiltonian (67) may include the crystalline field for spin $S = 5/2$. In the general case, where the crystalline field cannot be considered strong or weak compared to the exchange interaction, additional variational parameters are needed. For instance, a crystalline field of cubic symmetry splits the configuration $4f^1$ of the ion Ce^{+3} into the doublet Γ_7 and the quadruplet Γ_8. Then, to control the relative population of these two levels, we need one additional variational parameter. The model (67) of spin 1/2 can by used to analyze the heavy fermions in Li_2VO_4. As noted earlier, the electronic structure calculations done by Anisimov et al. [34] show that the states a_{1g} of spin 1/2 may be assumed to be localized, while the states e_g realize the half-filled d-band. Due to the Hund rule, there emerges a strong ferromagnetic exchange interaction J_{H} on a single site [34]. Taking the initial parameters from electronic structure calculations by the LDA + U method [34], i.e., $U = 3$ eV, the conduction band width $\Delta = 2$ eV, and $J = 1$ eV, we estimate the effective-mass renormalization coefficient q^{-1} at roughly 100, which agrees with the experimental data [32, 33]. We also note that the Hubbard model with the same parameters yields much smaller effective-mass values.

5. Conclusions

Experiments in magnetic neutron scattering point to the existence of short-range (nonlocal) order in almost all strongly correlated systems: classical strongly correlated metals, heavy-fermion compounds, and cuprate high-temperature superconductors. When a strongly correlated state is

destroyed by a magnetic field, temperature, or other factors, SRO also usually disappears. Strong short-range correlations can hardly be considered as being quasiparticle excitations, since they are poorly defined in momentum space and rapidly decay with the passage of time.

The methods used to study nonlocal correlations in quantum chemistry (small clusters and molecules) differ dramatically from those used in solid state physics (crystalline solids). In the first case, expansion in weakly excited states produces good results. In the second case, one needs a many-particle theory that takes SRO into account. The present review shows that microscopic models based on solutions for infinite-dimensional lattices (the variational Monte Carlo method, the $1/D + 1/D^2$ expansion of the Gutzwiller trial wave function, and DMFT) grossly underestimate the short-range nonlocal correlations in two- and three-dimensional lattices.

A variational theory that explicitly contains variational parameters corresponding to SRO has been developed. In the limit of an infinite-dimensional lattice, the solution obtained in the Hubbard model tends to the Gutzwiller solution, i.e., is practically an exact solution. In the opposite limit of a one-dimensional chain, the variational theory of SRO in the AFM phase yields a solution that is very close to the exact solution [13]. As $U \to 0$, the proposed theory passes to the band limit, while as $U \to \infty$ at half band-filling, it is in good agreement with the results of the Heisenberg model. The variational theory containing SRO parameters yields a significantly lower ground-state energy in the PM phase of the Hubbard model than the variational Monte Carlo method [20], which suggests that nonlocal correlations play a significant role. Coherent excited states form a narrow quasiparticle band which determines the thermodynamic properties of a strongly correlated system at low temperatures.

Calculations done in the framework of the Kondo–Hubbard model demonstrate the development of a coherent heavy-fermion state. Two types of behavior (Hubbard and Kondo-lattice) are distinguished here. In the Hubbard and Kondo–Hubbard models, the correlations whose range is larger than the distance between nearest neighbors obey the superposition hypothesis [1]. Hence their decay in coordinate space obeys an exponential law, which agrees with the experimental data discussed in Section 2. Note that in the case of a Kondo–Hubbard lattice this is not an obvious result, since the RKKY interaction between localized states falls off according to a power law rather than an exponential law.

The proposed variational theory can easily be generalized to incorporate more complicated models. For instance, to pass from the Hubbard model in the PM phase to an extended $U-J$ Hubbard model which contains additional exchange Ising interaction between neighboring sites, we must add only one term to the expression (55), $2J_{nn}(y_7 - y_6)$, where J_{nn} is the coupling constant. The main problem as the models get more complicated is the increase in the number of variational parameters. Calculations for 4 to 7 variational variables can be done on a personal computer. A further increase in the number of variables requires greater computational power. Hence the interest in simplified models, say, the $t-J$ model (27). Since in the $t-J$ model there are three states of a site, nine configurations of a site pair are possible. With allowance for normalization and self-consistency conditions, the number of independent variational parameters lowers to seven in any case (arbitrary band-filling, ferromagnetic and antiferromagnetic phases, magnetic field, etc.). Another way of overcoming the problem of the large number of variational parameters is to employ numerical methods, e.g., the variational Monte Carlo method, but on the trial wave function (28).

A number of problems concerning the proposed model of SRO are still unresolved. Among these is the problem of quasiparticle excitation spectra and the thermodynamics of SRO. Above, we only tentatively suggested ways of solving them. The present review did not discuss the problem of superconductivity in the variational model, since this problem merits a separate investigation. Superconducting phases can also be studied by the proposed theory if the initial wave function and the set of operators $\widehat{Y}_\lambda$ are properly chosen.

I am grateful to J Brooks and W Lewis for their attention to this work and for invaluable support. I would also like to express my gratitude to P Fulde for the hospitality during my stay at the Max-Plank-Institut für Komplexer Systeme. This work was partially supported by the International Science and Technology Center (Project No. 829).

References

1. Ziman J M *Models of Disorder*: *the Theoretical Physics of Homogeneously Disordered Systems* (Cambridge: Cambridge Univ. Press, 1979) [Translated into Russian (Moscow: Mir Publ., 1982)]
2. Mott N F *Metal–Insulator Transitions* (London: Taylor & Francis, 1974) [Translated into Russian (Moscow: Nauka, 1979)]
3. Hewson A C *The Kondo Problem to Heavy Fermions* (Cambridge: Cambridge Univ. Press, 1997)
4. Plakida N M *Vysokotemperaturnye Sverkhprovodniki* (High-Temperature Superconductors) (Moscow: Mezhdunarodnaya Programma Obrazovaniya, 1996) [Translated into English: *High-Temperature Superconductivity*: *Experiment and Theory* (Berlin: Springer, 1995)]
5. Bao W et al. *Phys. Rev. B* **58** 12727 (1998); cond-mat/9804320
6. Rossat-Mignod J et al. *J. Magn. Magn. Mater.* **76–77** 376 (1988)
7. Protogenov A P *Usp. Fiz. Nauk* **162** (7) 1 (1992) [*Sov. Phys. Usp.* **35** 535 (1992)]
8. Val'kov V V, Ovchinnikov S G *Kvazichastitsy v Sil'no Korrelirovannykh Sistemakh* (Quasiparticles in Strongly Correlated Systems) (Novosibirsk: Izd. SO RAN, 2001)
9. Izyumov Yu A *Usp. Fiz. Nauk* **165** 403 (1995) [*Phys. Usp.* **38** 385 (1995)]
10. Ovchinnikov S G *Usp. Fiz. Nauk* **167** 1043 (1997) [*Phys. Usp.* **40** 993 (1997)]
11. Senatore G, March N H *Rev. Mod. Phys.* **66** 445 (1994)
12. Georges A et al. *Rev. Mod. Phys.* **68** 13 (1996)
13. Lieb E H, Wu F Y *Phys. Rev. Lett.* **20** 1445 (1968)
14. Gebhard F *The Mott Metal–Insulator Transition*: *Models and Methods* (New York: Springer-Verlag, 1997)
15. Gutzwiller M C *Phys. Rev.* **134** A923 (1964); **137** A1726 (1965)
16. Zaĭtsev R O *Zh. Eksp. Teor. Fiz.* **75** 2362 (1978) [*Sov. Phys. JETP* **48** 1193 (1978)]
17. Metzner W, Vollhardt D *Phys. Rev. Lett.* **59** 121 (1987)
18. Metzner W, Vollhardt D *Phys. Rev. Lett.* **62** 324 (1989)
19. Metzner W *Z. Phys. B*: *Cond. Mat.* **77** 253 (1989)
20. Yokoyama H, Shiba H *J. Phys. Soc. Jpn.* **56** 1490, 3582 (1987)
21. Kudasov Yu B *Phys. Lett. A* **245** 153 (1998)
22. Kudasov Yu B *Zh. Eksp. Teor. Fiz.* **117** 624 (2000) [*JETP* **90** 544 (2000)]
23. Moriya T *Spin Fluctuations in Itinerant Electron Magnetism* (Berlin: Springer-Verlag, 1985) [Translated into Russian (Moscow: Mir, 1988)]
24. Raymond S et al. *J. Low Temp. Phys.* **109** 205 (1997)
25. Kuwamoto H, Honig J M, Appel J *Phys. Rev. B* **22** 2626 (1980)
26. Bugaev A A, Zakharchenya B P, Chudnovskiĭ F A *Fazovyĭ Perekhod Metall–Poluprovodnik i Ego Primenenie* (The Metal–Insulator Phase Transition and Its Application) (Leningrad: Nauka, 1979)

27. Brinkman W F, Rice T M *Phys. Rev. B* **2** 4302 (1970)
28. Bao W et al. *Phys. Rev. Lett.* **71** 766 (1993)
29. Park J-H et al. *Phys. Rev. B* **61** 11506 (2000)
30. Bao W et al. *J. Magn. Magn. Mater.* **177 – 181** 283 (1998)
31. Kondo S et al. *Phys. Rev. Lett.* **78** 3729 (1997)
32. Johnston D C *Physica B* **281** 21 (2000); cond-mat/9910404
33. Urano C et al. *Phys. Rev. Lett.* **85** 1052 (2000)
34. Anisimov V I et al. *Phys. Rev. Lett.* **83** 364 (1999); cond-mat/9903372
35. Fulde P et al., cond-mat/0101455
36. Lee S-H et al. *Phys. Rev. Lett.* **86** 5554 (2001)
37. Stewart G R, Fisk Z, Wire M S *Phys. Rev. B* **30** 482 (1984)
38. Tsujii H et al. *Phys. Rev. Lett.* **84** 5407 (2000)
39. Aeppli G et al. *Phys. Rev. Lett.* **57** 122 (1986)
40. Aeppli G, Busher E, Mason T E, in *Physical Phenomena at High Magnetic Fields* (Eds E Manousakis et al.) (Redwood City, Calif.: Addison-Wesley, 1992) p. 175
41. Aeppli G et al. *Phys. Rev. Lett.* **58** 808 (1987)
42. Goldman A I et al. *J. Magn. Magn. Mater.* **63 – 64** 380 (1987)
43. Bernhoeft N R, Lonzarich G G *J. Phys.: Condens. Matter* **7** 7325 (1995)
44. Regnault L P et al. *Phys. Rev. B* **38** 4481 (1988)
45. Broholm C et al. *Phys. Rev. Lett.* **58** 917 (1987)
46. Walter U, Wohleben D, Fisk Z *Z. Phys. B: Cond. Mat.* **62** 235 (1986)
47. Doniach S *Physica B + C* **91** 231 (1977)
48. Kambe S et al. *J. Phys. Soc. Jpn.* **65** 3294 (1996)
49. von Löhneysen H *J. Phys.: Condens. Matter* **8** 9689 (1996)
50. Sadovskiĭ M V *Usp. Fiz. Nauk* **171** 539 (2001) [*Phys. Usp.* **44** 515 (2001)]
51. Mason T E, cond-mat/9812287
52. Birgeneau R J et al., in *Mechanisms of High Temperature Superconductivity* (Springer Ser. in Materials Sci., Vol. 11, Eds H Kamimura, A Oshiyama) (Berlin: Springer-Verlag, 1989) p. 120
53. Bourges Ph "Spin dynamics in high-T_C cuprates", in *19th General Conf. of the Condensed Matter Division of the European Physical Society, Brighton, UK, 7 – 11 April 2002*, Europhysics Conf. Abstracts Vol. 26A (2002) p. 41; cond-mat/0009373
54. Bourges Ph et al., cond-mat/0006085
55. Fawcett E et al. *Phys. Rev. Lett.* **61** 558 (1988)
56. Hayden S M et al. *Phys. Rev. Lett.* **84** 999 (2000); cond-mat/9911442
57. Izyumov Yu A, Katsnel'son M I, Skryabin Yu N *Magnetizm Kollektivizirovannykh Elektronov* (Itinerant Electron Magnetism) (Moscow: Fizmatlit, 1994)
58. Sanchez-Castro C, Bedell K S, Cooper B R *Phys. Rev. B* **47** 6879 (1993)
59. Fazekas P *Lecture Notes on Electron Correlation and Magnetism* (Singapore: World Scientific, 1999)
60. Coqblin B et al. *J. Phys. Soc. Jpn.* **65** (Suppl. B) 64 (1996)
61. Lacroix C et al. *Physica B* **230 – 232** 503 (1997)
62. Rappoport T G, Figueira M S, Continentino M A *Phys. Lett. A* **264** 497 (2000); cond-mat/9904221
63. Fye R M, Hirsch J E *Phys. Rev. B* **40** 4780 (1989)
64. Kotliar G, Ruckenstein A E *Phys. Rev. Lett.* **57** 1362 (1986)
65. Trapper U, Ihle D, Fehske H *Phys. Rev. B* **52** R11553 (1995)
66. Ogawa T, Kanda K, Matsubara T *Prog. Theor. Phys.* **53** 614 (1975)
67. Vollhardt D *Rev. Mod. Phys.* **56** 99 (1984)
68. Fulde P *Electron Correlations in Molecules and Solids* 3rd ed. (Berlin: Springer-Verlag, 1995)
69. Gebhard F, Vollhardt D *Phys. Rev. Lett.* **59** 1472 (1987); *Phys. Rev. B* **38** 6911 (1988)
70. Gebhard F *Phys. Rev. B* **41** 9452 (1990)
71. Harris A B, Lange R V *Phys. Rev.* **157** 295 (1967)
72. Chao K A, Spalek J, Oles A M *J. Phys. C: Solid State Phys.* **10** L271 (1977)
73. Gros C, Joynt R, Rice T M *Phys. Rev. B* **36** 381 (1987)
74. Izyumov Yu A *Usp. Fiz. Nauk* **167** 465 (1997) [*Phys. Usp.* **40** 445 (1997)]
75. Horsch P, Fulde P *Z. Phys. B: Cond. Mat.* **36** 23 (1979)
76. Stollhoff G, Fulde P *Z. Phys. B: Cond. Mat.* **29** 231 (1978)
77. Stollhoff G, Fulde P *Z. Phys. B: Cond. Mat.* **26** 257 (1977)
78. Razafimandimby H A *Z. Phys. B: Cond. Mat.* **49** 33 (1982)
79. Kubo R *J. Phys. Soc. Jpn.* **17** 1100 (1962)
80. Stollhoff G, Fulde P *J. Chem. Phys.* **73** 4548 (1980)
81. Rościszewski K, Chaumet M, Fulde P *Chem. Phys.* **143** 47 (1990)
82. Kikuchi R *Phys. Rev.* **81** 988 (1951)
83. Kikuchi R, Brush S G *J. Chem. Phys.* **47** 195 (1967)
84. Kikuchi R *Prog. Theor. Phys. Suppl.* **115** 1 (1995)
85. Morita T *Prog. Theor. Phys. Suppl.* **115** 27 (1995)
86. Tanaka G, Kimura M *Prog. Theor. Phys. Suppl.* **115** 207 (1995)
87. Pelizzola A *Phys. Rev. B* **61** 11510 (2000)
88. Cenedese P, Cahn J W *Prog. Theor. Phys. Suppl.* **115** 95 (1995)
89. Ishii T *J. Phys. Soc. Jpn.* **69** 139 (2000)
90. Wada K, Kaburagi M *Prog. Theor. Phys. Suppl.* **115** 273 (1995)
91. An G *J. Stat. Phys.* **52** 727 (1988)
92. Morita T *J. Stat. Phys.* **59** 819 (1990)
93. Hubbard J *Proc. R. Soc. London Ser. A* **281** 401 (1964)
94. Manousakis E *Rev. Mod. Phys.* **63** 1 (1991)
95. Thomas G A et al. *Phys. Rev. Lett.* **73** 1529 (1994)
96. des Cloizeaux J *J. Phys.* (Paris) **20** 606 (1959)
97. Plakida N M, Oudovenko V S *Phys. Rev. B* **59** 11949 (1999)
98. Plakida N M et al., cond-mat/0104234
99. Kudasov Yu B *Fiz. Tverd. Tela* **43** 1491 (2001) [*Phys. Solid State* **43** 1552 (2001)]
100. Schork T, Blawid S, Igarashi J *Phys. Rev. B* **59** 9888 (1999)
101. Kudasov Yu B, cond-mat/0012018
102. Kudasov Yu B *Zh. Eksp. Teor. Fiz.* **109** 174 (1996) [*JETP* **82** 92 (1996)]
103. Kudasov Yu B *Fiz. Tverd. Tela* **38** 1335 (1996) [*Phys. Solid State* **38** 739 (1996)]
104. Hubbard J *Proc. R. Soc. London Ser. A* **276** 238 (1963)
105. Zubarev D N *Usp. Fiz. Nauk* **71** 71 (1960) [*Sov. Phys. Usp.* **3** 320 (1960)]
106. Fulde P *Ann. Phys.* (Leipzig) **9** 871 (2000)
107. Lavagna M, Pepin C, in *Proc. of the XXXVIII Cracow School of Theoretical Physics, Zakopane, Poland, June 1 – 10, 1998*; *Acta Phys. Pol. B* **29** 3753 (1998); cond-mat/9903093